

# Torus Probabilistic Principal Component Analysis

Anahita Nodehi, Mousa Golalizadeh<sup>†</sup>, Mehdi Maadooliat,  
Claudio Agostinelli

---

<sup>0</sup> **Anahita Nodehi:**

Department of Statistics, Tarbiat Modares University, Tehran, Iran.  
Department of Statistics, Computer Science, Applications, University of Florence,  
Florence, Italy.  
`anahita.nodehi@unifi.it`

<sup>†</sup> **Mousa Golalizadeh**(Corresponding author):

Department of Statistics, Tarbiat Modares University, Tehran, Iran.  
`golalizadeh@modares.ac.ir`

**Mehdi Maadooliat:**

Department of Statistics, Marquette University, Milwaukee, USA.  
`mehdi.maadooliat@marquette.edu`

**Claudio Agostinelli:**

Department of Mathematics, University of Trento, Trento, Italy.  
`claudio.agostinelli@unitn.it`

## Abstract

One of the most common problems that any technique encounters is the high dimensionality of the input data. This yields several problems in the subsequently performed statistical methods due to the so-called “curse of dimensionality”. Several dimension reduction methods have been proposed in the literature, until now, to accomplish the goal of having a smaller dimensional space. The most popular among them, is the so-called Principal Component Analysis (PCA). One of the extensions of PCA is Probabilistic PCA (known as PPCA). In PPCA, a probabilistic model is used to perform the dimension reduction. By convention, there are cases in applied sciences, e.g. bioinformatics, biology and geology that the data at hand are in non-Euclidean space. Elaborating further, an important situation is when each variable poses a direction so that a data point is lying on a torus. According to its importance, the extension of the PCA to such data is being under attention during last decades. In this paper, we introduce a Probabilistic PCA for data in torus (TPPCA), assuming a multivariate wrapped normal distribution as the underline model. Further, we present certain appropriate algorithms to compute this dimension reduction technique and then, we compare our proposal with other dimension reduction techniques using examples based on real datasets and a small Monte Carlo simulation.

**keyword:** Principal Component Analysis; Probabilistic Principal Component Analysis; Non-Euclidean Space; Directional Data; Torus; Wrapped Normal distribution.

## 1 Introduction

There are several difficulties that can arise in high dimensions which are summarized under the named “curse of dimensionality” [Bellman, 1961]. In this regard, the Principal Component Analysis (PCA) is one of the classical method to overcome problems arising in such cases. This method was first introduced by Pearson [1901], and developed independently by Hotelling [1933]. Similar to many multivariate methods, it was not widely used until the advent of electronic computers. The main idea of PCA is to reduce the dimensionality of a data set in which there are a large number of correlated variables, retaining as much of the variation presented in the data set as

possible [Jolliffe, 2002]. Classic PCA lacks of a probability model and the associated likelihood measure. Considering this, a probabilistic formulation is sometime appealing because the definition of a likelihood measure enables comparison with other probabilistic techniques. Moreover, it facilitates the statistical testing and permits the application of Bayesian methods. Furthermore, the inference about missing data [Tipping and Bishop, 1997] can then be enabled.

Directional data are often the result of experiments in applied sciences e.g. biology, geology, bioinformatics and etc. It is common to specify such measures as an angle on a unit circle once an initial direction and orientation of the circle have been chosen. The statistical analysis of these angles are named directional statistics [Mardia, 1972]. Some authors named directional data as “circular data” or “angular data”. Accordingly, these types of data are also part of the so called “non-Euclidean data” or “manifold-valued data”. There have been many attempts to extend PCA on manifold data. To name but a few: Principal Curve [Hastie and Stuetzle, 1989], Principal Geodesic Analysis (PGA) [Fletcher et al., 2004], Geodesic Principal Component Analysis (GPCA) [Huckemann and Ziezold, 2006], dihedral angles Principal Component Analysis (dPCA) (Mu et al. [2005] and Altis et al. [2007]), Principal Arc Analysis (PAA) [Jung et al., 2010], Principal Nested Analysis (PNS) [Jung et al., 2012], Principal Flows (PF) [Panaretos et al., 2014], dihedral angles Principal Geodesic Analysis [Nodehi et al., 2015], Torus Principal Component Analysis (TPCA) [Eltzner et al., 2018] and PCA on torus (dPCA+) [Sittel et al., 2017]. Such dimension reduction methods are not based upon a probabilistic model. Zhang and Fletcher [2013] proposed a latent variable model, named Probabilistic PGA which is an extension of Probabilistic PCA on sphere. Accordingly, they demonstrated the ability of this method to recover the parameters in simulated sphere data. Following this method, they measured the ability and effectiveness in analyzing shape variability of a corpus callosum data set from human brain images. Here, we introduce the Torus Probabilistic PCA (TPPCA) which is an extension of the PPCA on torus using the multivariate wrapped normal model.

Section 2 describes Principal Component Analysis (PCA) and its extensions in non-Euclidean space. Section 3 illustrates an extension of PCA based on probabilistic model. Section 4 introduces the Torus Probabilistic Principal Component Analysis while Section 5 discusses the selection of number of components. Section 6 reports the results of a small Monte Carlo simulation and an illustrative example based on real datasets is presented in Section 7.

Section 8 proposes final comments and remarks. A Supplementary Material is available and in Section SM-2, it contains details on how to estimate the parameters in PPCA model; in Section SM-3 descriptions of the Classification EM algorithm used to perform estimation in the multivariate wrapped normal model is illustrated; and in Section SM-6 the complete analysis for a real data of RNA in 7-torus space is reported.

## 2 Principal Component Analysis and its extensions in non-Euclidean space

Principal component analysis (PCA), is a technique that is widely used for applications such as dimensionality reduction, lossy data compression, feature extraction, and data visualization [Jolliffe, 2002]. There are two formulations of PCA that give rise to the same algorithm. First, PCA can be defined as the orthogonal projection of the data onto a lower dimensional linear space, known as the principal subspace, such that the variance of the projected data is maximized [Hotelling, 1933]. Second, it can be defined as the linear projection that minimizes the average projection cost, defined as the mean squared distance between the data points and their projections. Further, it builds a linear transformation of variables in such way that new combined variables are nearly uncorrelated [Pearson, 1901].

A non-Euclidean space can be identified with various distinct bases [Karcher, 1977], so that the distance among points is a function of those bases. One can define different similarity measures to describe differences among variables. Consequently, the PCA based on these distances, while ignoring the topological feature of non-Euclidean space, can be invoked. This, in fact, returns back to bases (variables) considered to construct the space to work with.

Direction measurements are often the result of experiments in many scientific fields. For instance, a biologist may be measuring the direction of flight of a bird or the orientation of an animal. Directional data can be specified by an angle on a unit circle once an initial direction and orientation of the circle have been chosen. The statistical analysis of angles is closely linked to the statistics on manifold [Pennec, 2006, Karcher, 1977]. Clearly, using linear statistics directly on angles is cumbersome. To get a statistical measure of variability on any manifold using manifold-valued data, we need

to compute the length of paths by a Riemannian metric [Karcher, 1977]. In order to perform statistical analysis on a manifold, it is often common to approximate the manifold by a linearized space and undertake most of the analysis there and project the results back. However, there are many advantages of using mathematical tools directly on the Riemannian manifold rather than invoking any approximation procedure [Pennec, 2006].

We describe three recent techniques for torus data, in Section SM-1 of the Supplementary Material we provide a description of other available methods for torus data.

### **Torus Principal Component Analysis (TPCA)**

Eltzner et al. [2018] extends classic PCA to torus data (TPCA). This method is deforming tori into spheres and then, uses a variant of the recently developed Principal Nested Analysis [Jung et al., 2012] to perform the dimensional reduction. Moreover, TPCA analysis involves a step of small sphere fitting and they provide an improved test to avoid over-fitting. However, deforming tori into spheres creates singularities. Thus, they introduce a data-adaptive pre-clustering technique to avoid singularities. Subsequently, they illustrate this method with two recently studied RNA structures.

### **PCA on torus (dPCA+)**

Sittel et al. [2017] introduced dPCA+ as an extension of dPCA with application to protein data. The main idea is that the (periodicity-induced) projection error can be minimized by transforming the data such that the maximal gap of the sampling is shifted to the periodic boundary. For the second step, the covariance matrix and its Eigen-decomposition can be computed in a standard manner. This method respects the special topology of the torus by preserving the correct neighborhoods of the data points. Further, dPCA+ yields directly certain interpretable covariance matrices and eigenvectors, which readily reveal the contributions of the various circular variables. In this regard, the main assumption underlying dPCA+ is that the data indeed show a significant gap in their distribution which is, in general, a limitation.

### Probabilistic Principal Geodesic Analysis (PPGA)

Principal Geodesic Analysis (PGA) is a generalization of PCA to nonlinear manifolds. It describes the geometric variability of manifold data by finding the lower-dimensional geodesic subspaces that minimize the residual sum-of-squared geodesic distances to the data. Similar to PCA, current dimension reduction method on manifolds lack a probabilistic interpretation. In another study conducted by Zhang and Fletcher [2013], they proposed a latent variable model for PGA, called Probabilistic PGA (PPGA). This method is an extension of PPCA on manifolds. Due to the lack of an explicit formulation for the normalizing constant, this estimation is limited to symmetric spaces, which include many common manifolds such as Euclidean space, spheres, Kendall shape spaces, Grassman or Stiefel manifolds, and so forth. Analogous to PPCA, this method recovers low-dimensional factors as maximum likelihood. To compute the maximum likelihood estimates of the parameters in the model, they developed a Monte Carlo Expectation Maximization algorithm, where the expectation is approximated by Hamiltonian Monte Carlo sampling of the latent variables. Furthermore, Zhang and Fletcher [2015] proposed a Bayesian inference procedure for model parameter estimation and simultaneous detection of the effective dimensionality of the latent space.

## 3 Probabilistic Principal Component Analysis

The definition of PCA discussed in the previous section was based on a linear projection of the data onto a subspace of lower dimensionality than the original data space. Probabilistic PCA (PPCA) is an extension of PCA which can also be expressed as the maximum likelihood solution of a probabilistic latent variable model. PPCA was proposed independently by Tipping and Bishop [1997, 1999] and Roweis [1998]. It is worth to note that Probabilistic PCA is closely related to Factor Analysis [Basilevsky, 1994].

Probabilistic PCA brings several advantages compared with PCA. Using probabilistic model with the definition of a likelihood measure enables comparison with other probabilistic techniques using statistical testing and allow the application of Bayesian methods. Moreover, the combination of a probabilistic model and EM slgorithms allows us to deal with missing values

in the data set. Further, this Probabilistic PCA can also be used to model class-conditional densities and hence be applied to classification problems.

A latent variable model seeks to relate a  $D$ -dimensional observation vector  $\mathbf{X}$  to a corresponding  $d$ -dimensional vector of latent (or unobserved) variables  $\mathbf{Z}$  ( $d < D$ ), using the model

$$\mathbf{X} = \boldsymbol{\mu} + W\mathbf{Z} + \boldsymbol{\epsilon}$$

where  $\mathbf{X} = (X_1, \dots, X_D)^\top$ ,  $\mathbf{Z} \sim N(\mathbf{0}, I_d)$  is an  $d$ -dimensional Gaussian latent variable, and  $\boldsymbol{\epsilon} \sim N(\mathbf{0}, \sigma^2 I_D)$  is a  $D$ -dimensional zero-mean Gaussian-distributed noise variable with covariance  $\sigma^2 I_D$ . Assuming  $\text{Cov}(\mathbf{Z}, \boldsymbol{\epsilon}) = \mathbf{0}$  we obtain,

$$\mathbb{E}(\mathbf{X}) = \mathbb{E}(\boldsymbol{\mu} + W\mathbf{Z} + \boldsymbol{\epsilon}) = \boldsymbol{\mu}$$

and

$$\text{Cov}(\mathbf{X}) = \mathbb{E}[(\boldsymbol{\mu} + W\mathbf{Z} + \boldsymbol{\epsilon})(\boldsymbol{\mu} + W\mathbf{Z} + \boldsymbol{\epsilon})^\top] = WW^\top + \sigma^2 I_D = C.$$

As suggested in Tipping and Bishop [1997] there are two ways to estimate the parameters: matrix decomposition and Expectation-Maximization algorithm (EM). One of the benefits of the EM algorithm for PPCA is computational efficiency in large-scale applications [Roweis, 1998]. Another feature of the EM approach is that we can take the limit  $\sigma^2 \rightarrow 0$  corresponding to standard PCA, and still obtain a valid EM-like algorithm [Roweis, 1998]. In Section SM-2 of the Supplementary Material, one can find a review of both procedures.

## 4 Torus Probabilistic Principal Component Analysis

Probabilistic PCA is an extension of PCA which is expressed as the maximum likelihood solution of a probabilistic latent variable model. Here, we focus on the extension of PPCA to torus data. Let  $X \in \mathbb{R}$  be a real random variable, a circular random variable  $Y$  might be written as  $Y = X \bmod 2\pi \in [0, 2\pi)$  or  $X = Y + 2\pi K$  for some  $K \in \mathbb{Z}$ . Let  $\mathbb{T}^D = [0, 2\pi)^D$  be the  $D$ -torus. According to the above-description, we consider a latent variable model that seeks to relate a  $D$ -dimensional observation vector  $\mathbf{Y} \in \mathbb{T}^D$  to a corresponding  $d$ -dimensional vector of latent (or unobserved) variables  $\mathbf{Z} \in \mathbb{R}^d$  ( $d < D$ ), that

is,

$$\begin{aligned} \mathbf{Y} &= \mathbf{X} \bmod 2\pi \\ \mathbf{X} &= \boldsymbol{\mu} + W\mathbf{Z} + \boldsymbol{\epsilon} \end{aligned} \tag{1}$$

where  $\mathbf{Y} = (Y_1, \dots, Y_D)^\top$ ,  $\mathbf{X} = (X_1, \dots, X_D)^\top$ ,  $\mathbf{Z} \sim N_d(\mathbf{0}, I_d)$  is an  $d$ -dimensional Gaussian latent variable and  $\boldsymbol{\epsilon} \sim N_D(\mathbf{0}, \sigma^2 I_D)$  is a  $D$ -dimensional zero-mean Gaussian-distributed noise variable with covariance  $\sigma^2 I_D$ . We assume  $\text{Cov}(\mathbf{Z}, \boldsymbol{\epsilon}) = 0$  and there exists a vector  $\mathbf{K}$  such that  $\mathbf{Y} = \mathbf{X} - 2\pi\mathbf{K} \in \mathbb{T}^D$ . We recall the following basic results [Mardia et al., 1979]

$$\begin{aligned} \mathbf{X} &\sim N_D(\boldsymbol{\mu}, WW^\top + \sigma^2 I_D) \\ \mathbf{X}|\mathbf{Z} &\sim N_D(\boldsymbol{\mu} + W\mathbf{Z}, \sigma^2 I_D) \\ \mathbf{Z}|\mathbf{X} &\sim N_d(M^{-1}W^\top(\mathbf{X} - \boldsymbol{\mu}), \sigma^2 M^{-1}) , \\ \mathbf{Z}|\mathbf{Y} + 2\pi\mathbf{K} &\sim N_d(M^{-1}W^\top(\mathbf{Y} + 2\pi\mathbf{K} - \boldsymbol{\mu}), \sigma^2 M^{-1}) . \end{aligned} \tag{2}$$

where  $M = W^\top W + \sigma^2 I_d$ . For a given point  $\mathbf{x} \in \mathbb{R}^D$  we define a parameter vector  $\mathbf{k} \in \mathbb{Z}^D$  so that  $\mathbf{y} = \mathbf{x} - 2\pi\mathbf{k} \in \mathbb{T}^D$ , then

$$f(\mathbf{y}, \mathbf{x}, \mathbf{z}, \mathbf{k}) = f(\mathbf{y}|\mathbf{x}, \mathbf{z}, \mathbf{k})f(\mathbf{x}|\mathbf{z})f(\mathbf{z}) = f(\mathbf{y}|\mathbf{x}, \mathbf{k})f(\mathbf{x}|\mathbf{z})f(\mathbf{z})$$

where

$$f(\mathbf{y}|\mathbf{x}, \mathbf{k}) = \mathbb{1}_T(\mathbf{y}, \mathbf{x}, \mathbf{k}) = \begin{cases} 1 & \text{if } \mathbf{y} = \mathbf{x} - 2\pi\mathbf{k} \in \mathbb{T}^D \\ 0 & \text{otherwise} \end{cases}$$

which leads to the joint distribution

$$\begin{aligned} f(\mathbf{y}, \mathbf{x}, \mathbf{z}, \mathbf{k}) &\propto \mathbb{1}_T(\mathbf{y}, \mathbf{x}, \mathbf{k})(\sigma^2)^{-\frac{D}{2}} \exp \left\{ -\frac{(\mathbf{y} + 2\pi\mathbf{k} - W\mathbf{z} - \boldsymbol{\mu})^\top (\mathbf{y} + 2\pi\mathbf{k} - W\mathbf{z} - \boldsymbol{\mu})}{2\sigma^2} \right. \\ &\quad \left. -\frac{\mathbf{z}^\top \mathbf{z}}{2} \right\} . \end{aligned}$$



Let  $\mathcal{Y} = (\mathbf{y}_1, \dots, \mathbf{y}_N)$  be a sample of size  $N$  and let  $\mathcal{K} = (\mathbf{k}_1, \dots, \mathbf{k}_N)$  a set of unknown parameters, then log-likelihood function is given by

$$\begin{aligned}
\ell(\boldsymbol{\mu}, W, \sigma^2, \mathcal{K}) &= \sum_{j=1}^N \ln f(\mathbf{y}_j, \mathbf{x}_j, \mathbf{z}_j, \mathbf{k}_j) \\
&\propto \sum_{j=1}^N \left[ -\frac{D}{2} \ln \sigma^2 - \frac{(\mathbf{x}_j - W\mathbf{z}_j - \boldsymbol{\mu})^\top (\mathbf{x}_j - W\mathbf{z}_j - \boldsymbol{\mu})}{2\sigma^2} - \frac{\mathbf{z}_j^\top \mathbf{z}_j}{2} \right] \\
&\quad \times \mathbb{1}_T(\mathbf{y}_j, \mathbf{x}_j, \mathbf{k}_j) \\
&\propto \sum_{j=1}^N \left[ -D \ln \sigma^2 - \frac{\text{tr}[(\mathbf{y}_j + 2\pi\mathbf{k}_j - \boldsymbol{\mu})(\mathbf{y}_j + 2\pi\mathbf{k}_j - \boldsymbol{\mu})^\top]}{\sigma^2} \right. \\
&\quad \left. + 2 \frac{(\mathbf{y}_j + 2\pi\mathbf{k}_j - \boldsymbol{\mu})\mathbf{z}_j^\top W^\top}{\sigma^2} - \frac{\text{tr}[(W\mathbf{z}_j)(W\mathbf{z}_j)^\top]}{\sigma^2} - \text{tr}(\mathbf{z}_j\mathbf{z}_j^\top) \right] \\
&\quad \times \mathbb{1}_T(\mathbf{y}_j, \mathbf{x}_j, \mathbf{k}_j)
\end{aligned}$$

where in the last line we use the fact  $\text{tr}(AB) = \text{tr}(BA)$ . We are going to take expectation of the log-likelihood over the latent variables  $\mathbf{Z}_1, \dots, \mathbf{Z}_N$  given

the data sample  $\mathcal{Y}$ , that is,

$$\begin{aligned}
\Gamma(\boldsymbol{\mu}, W, \sigma^2, \mathcal{K} | \mathcal{Y}) &= \mathbb{E}(\ell | \mathcal{Y}) = \sum_{j=1}^N \mathbb{E}(\ell(\boldsymbol{\mu}, W, \sigma^2, \mathcal{K}) | \mathbf{Y}_j = \mathbf{y}_j) \\
&\propto \sum_{j=1}^N \left\{ -D \ln \sigma^2 - \text{tr}[\mathbb{E}(\mathbf{Z}_j \mathbf{Z}_j^\top | \mathbf{Y}_j = \mathbf{y}_j)] \right. \\
&\quad - \frac{(\mathbf{y}_j + 2\pi \mathbf{k}_j - \boldsymbol{\mu})(\mathbf{y}_j + 2\pi \mathbf{k}_j - \boldsymbol{\mu})^\top}{\sigma^2} \\
&\quad + 2 \frac{(\mathbf{y}_j - \boldsymbol{\mu} + 2\pi \mathbf{k}_j) \mathbb{E}(\mathbf{Z}_j^\top | \mathbf{Y}_j = \mathbf{y}_j) W^\top}{\sigma^2} \\
&\quad \left. - \frac{\text{tr}[W \mathbb{E}(\mathbf{Z}_j \mathbf{Z}_j^\top | \mathbf{Y}_j = \mathbf{y}_j) W^\top]}{\sigma^2} \right\} \\
&\times \mathbb{1}_T(\mathbf{y}_j, \mathbf{x}_j, \mathbf{k}_j) \\
&= \sum_{j=1}^N \left\{ -D \ln \sigma^2 - \text{tr}[\mathbb{E}(\mathbf{Z}_j \mathbf{Z}_j^\top | \mathbf{X}_j = \mathbf{y}_j + 2\pi \mathbf{k}_j)] \right. \\
&\quad - \frac{(\mathbf{y}_j + 2\pi \mathbf{k}_j - \boldsymbol{\mu})^\top (\mathbf{y}_j + 2\pi \mathbf{k}_j - \boldsymbol{\mu})}{\sigma^2} \\
&\quad - \frac{\text{tr}[W \mathbb{E}(\mathbf{Z}_j \mathbf{Z}_j^\top | \mathbf{X}_j = \mathbf{y}_j + 2\pi \mathbf{k}_j) W^\top]}{\sigma^2} \\
&\quad \left. + 2 \frac{(\mathbf{y}_j + 2\pi \mathbf{k}_j - \boldsymbol{\mu}) \mathbb{E}(\mathbf{Z}_j^\top | \mathbf{X}_j = \mathbf{y}_j + 2\pi \mathbf{k}_j) W^\top}{\sigma^2} \right\} \\
&\times \mathbb{1}_T(\mathbf{y}_j, \mathbf{x}_j, \mathbf{k}_j) ,
\end{aligned}$$

where in the last line, given a function  $g(\cdot)$  and the definition of  $\mathbf{k}$  we can see that

$$\mathbb{E}(g(\mathbf{Z}) | \mathbf{Y} = \mathbf{y}) = \mathbb{E}(g(\mathbf{Z}) | \mathbf{X} = \mathbf{y} + 2\pi \mathbf{k}) .$$

Considering this description, the TPPCA can be described as a two steps algorithm, in the first step given values for  $W$  and  $\sigma^2$  we update the estimates of  $\boldsymbol{\mu}$  and  $\mathcal{K}$ , in the second step, given values for  $\boldsymbol{\mu}$  and  $\mathcal{K}$  we update the estimates of  $W$  and  $\sigma^2$ . Initial values for all the parameters are given by a procedure described in Section 4.3.

## 4.1 Step 1

Updating  $\boldsymbol{\mu}$  and  $\mathcal{K}$  can be done as in Nodehi et al. [2020] using a Classification Expectation Maximization algorithm (CEM), see Section SM-3 for a short review of the procedure. Considering  $\Gamma(\boldsymbol{\mu}, \hat{W}, \hat{\sigma}^2, \mathcal{K}|\mathcal{Y})$ , the CEM algorithm is an iterative classification algorithm which estimates the parameters (in our case  $\boldsymbol{\mu}$ ) and the classification (in our case  $\mathcal{K}$ ), simultaneously.

- **E step (Expectation):** Given a value  $\hat{\boldsymbol{\mu}}$ , compute the expectation  $\Gamma(\hat{\boldsymbol{\mu}}, \hat{W}, \hat{\sigma}^2, \mathcal{K}|\mathcal{Y})$ ;
- **C step (Classification):** Update  $\hat{\mathcal{K}}$  by

$$\hat{\mathcal{K}} = \arg \max_{\mathcal{K}} \sum_{j=1}^N \Gamma(\hat{\boldsymbol{\mu}}, \hat{W}, \hat{\sigma}^2, \mathcal{K}|\mathcal{Y}) = \arg \max_{\mathbf{k}_j, j=1, \dots, N} \sum_{j=1}^N \Gamma(\hat{\boldsymbol{\mu}}, \hat{W}, \hat{\sigma}^2, \mathbf{k}_j|\mathbf{y}_j), \quad ,$$

which is equivalent to maximizing component by component  $\Gamma(\hat{\boldsymbol{\mu}}, \hat{W}, \hat{\sigma}^2, \mathbf{k}_j|\mathbf{y}_j)$  i.e.

$$\hat{\mathbf{k}}_j = \arg \max_{\mathbf{k}_j \in \mathbb{Z}^D} \Gamma(\hat{\boldsymbol{\mu}}, \hat{W}, \hat{\sigma}^2, \mathbf{k}_j|\mathbf{y}_j), \quad j = 1, \dots, N.$$

- **M step (Maximization):** Using (2), and considering  $\Gamma(\boldsymbol{\mu}, \hat{W}, \hat{\sigma}^2, \hat{\mathcal{K}}|\mathcal{Y})$  we update  $\hat{\boldsymbol{\mu}}$  by evaluating

$$\begin{aligned} \frac{\partial \Gamma(\boldsymbol{\mu}, \hat{W}, \hat{\sigma}^2, \hat{\mathcal{K}}|\mathcal{Y})}{\partial \boldsymbol{\mu}} &= \sum_{j=1}^N \left[ \frac{(\mathbf{y}_j + 2\pi \hat{\mathbf{k}}_j - \boldsymbol{\mu})^\top}{\sigma^2} - \frac{\mathbb{E}(\mathbf{Z}_j^\top | \mathbf{y}_j + 2\pi \hat{\mathbf{k}}_j) W^\top}{\sigma^2} \right] \\ &= \sigma^{-2} \sum_{j=1}^N (\mathbf{y}_j + 2\pi \hat{\mathbf{k}}_j - \boldsymbol{\mu})^\top - \sum_{j=1}^N (\mathbf{y}_j + 2\pi \hat{\mathbf{k}}_j - \boldsymbol{\mu})^\top W M^{-1} W^\top, \end{aligned}$$

equating it to  $\mathbf{0}$  and solving for  $\boldsymbol{\mu}$  leads to

$$N \boldsymbol{\mu}^\top (I_D - W M^{-1} W^\top) = \sum_{j=1}^N (\mathbf{y}_j + 2\pi \hat{\mathbf{k}}_j)^\top (I_D - W M^{-1} W^\top)$$

that is

$$\hat{\boldsymbol{\mu}} = \frac{\sum_{j=1}^N (\mathbf{y}_j + 2\pi \hat{\mathbf{k}}_j)}{N} = \frac{\sum_{j=1}^N \hat{\mathbf{x}}_j}{N}$$

where  $\hat{\mathbf{x}}_j = \mathbf{y}_j + 2\pi \hat{\mathbf{k}}_j$  is an estimates of the unobserved  $\mathbf{x}_j$  ( $j = 1, \dots, N$ ).

## 4.2 Step 2

Considering the derivative of  $\Gamma(\hat{\boldsymbol{\mu}}, W, \sigma^2, \hat{\mathcal{K}}|\mathcal{Y})$  with respect to  $W$  and  $\sigma^2$ , that is

$$\frac{\partial \Gamma(\hat{\boldsymbol{\mu}}, W, \sigma^2, \hat{\mathcal{K}}|\mathcal{Y})}{\partial W} = \sum_{j=1}^N \left[ -\frac{W \mathbb{E}(\mathbf{Z}_j \mathbf{Z}_j^\top | \hat{\mathbf{x}}_j)}{2\sigma^2} + \sigma^{-2} (\hat{\mathbf{x}}_j - \hat{\boldsymbol{\mu}}) \mathbb{E}(\mathbf{Z}_j^\top | \hat{\mathbf{x}}_j) \right]$$

we obtain

$$\begin{aligned} \hat{W} &= \left[ \sum_{j=1}^N (\hat{\mathbf{x}}_j - \hat{\boldsymbol{\mu}}) \mathbb{E}(\mathbf{Z}_j^\top | \hat{\mathbf{x}}_j) \right] \left[ \sum_{j=1}^N \mathbb{E}(\mathbf{Z}_j \mathbf{Z}_j^\top | \hat{\mathbf{x}}_j) \right]^{-1} \\ &= \left[ \sum_{j=1}^N (\hat{\mathbf{x}}_j - \hat{\boldsymbol{\mu}}) (\hat{\mathbf{x}}_j - \hat{\boldsymbol{\mu}})^\top W M^{-1} \right] \left[ N\sigma^2 M^{-1} + \sum_{j=1}^N M^{-1} W^\top (\hat{\mathbf{x}}_j - \hat{\boldsymbol{\mu}}) (\hat{\mathbf{x}}_j - \hat{\boldsymbol{\mu}})^\top W M^{-1} \right]^{-1} \\ &= S W M^{-1} \{ \sigma^2 M^{-1} + (M^{-1} W^\top S W M^{-1}) \}^{-1} \\ &= S W M^{-1} M (\sigma^2 I_d + M^{-1} W^\top S W)^{-1} \\ &= S W (\sigma^2 I_d + M^{-1} W^\top S W)^{-1} \end{aligned}$$

where  $S = \frac{1}{N} \sum_{j=1}^N (\hat{\mathbf{x}}_j - \hat{\boldsymbol{\mu}}) (\hat{\mathbf{x}}_j - \hat{\boldsymbol{\mu}})^\top$  has the same shape as the usual Maximum Likelihood Estimates of the variance and covariace matrix for the (estimated) sample  $\hat{\mathbf{x}}_1, \dots, \hat{\mathbf{x}}_N$  with estimated mean vector  $\hat{\boldsymbol{\mu}}$ .

After substituting  $\hat{W}$  in  $\Gamma(\hat{\boldsymbol{\mu}}, \hat{W}, \sigma^2, \hat{\mathcal{K}}|\mathcal{Y})$  and using (2), the estimating equation of  $\sigma^2$  is

$$\begin{aligned} \frac{\partial \Gamma(\hat{K}, \hat{W}, \sigma^2, \hat{\boldsymbol{\mu}}|Y)}{\partial \sigma^2} &= \sum_{j=1}^N -\frac{D}{\sigma^2} - \frac{1}{\sigma^4} \left[ \text{tr}[(\hat{\mathbf{x}}_j - \hat{\boldsymbol{\mu}}) (\hat{\mathbf{x}}_j - \hat{\boldsymbol{\mu}})^\top] \right. \\ &\quad \left. - \text{tr}(\hat{W} \mathbb{E}(\mathbf{Z}_j \mathbf{Z}_j^\top | \hat{\mathbf{x}}_j) \hat{W}^\top) \right] - \frac{2}{\sigma^4} \left[ (\hat{\mathbf{x}}_j - \hat{\boldsymbol{\mu}}) \mathbb{E}(\mathbf{Z}_j^\top | \hat{\mathbf{x}}_j) \hat{W}^\top \right] = 0 \end{aligned}$$

which leads to

$$\begin{aligned}
\hat{\sigma}^2 &= \frac{1}{ND} \sum_{j=1}^N \left[ \text{tr}[(\hat{\mathbf{x}}_j - \hat{\boldsymbol{\mu}})(\hat{\mathbf{x}}_j - \hat{\boldsymbol{\mu}})^\top] - 2(\hat{\mathbf{x}}_j - \hat{\boldsymbol{\mu}}) \mathbb{E}(\mathbf{Z}_j^\top | \hat{\mathbf{x}}_j) \hat{W}^\top - \text{tr}(\hat{W} \mathbb{E}(\mathbf{Z}_j \mathbf{Z}_j^\top | \hat{\mathbf{x}}_j)) \hat{W}^\top \right] \\
&= \frac{1}{D} \text{tr}[S - 2SWM^{-1}\hat{W}^\top + \hat{W}(\sigma^2 M^{-1} + M^{-1}W^\top SWM^{-1})\hat{W}^\top] \\
&= \frac{1}{D} \text{tr}[S - 2SWM^{-1}\hat{W}^\top + \hat{W}(\sigma^2 I_d + M^{-1}W^\top SW)M^{-1}\hat{W}^\top] \\
&= \frac{1}{D} \text{tr}[S - 2SWM^{-1}\hat{W}^\top + \hat{W}\hat{W}^{-1}SWM^{-1}\hat{W}^\top] \\
&= \frac{1}{D} \text{tr}[S - SWM^{-1}\hat{W}^\top] .
\end{aligned}$$

### 4.3 Initial values

Hereafter, we describe how to obtain suitable initial values for  $\boldsymbol{\mu}$ ,  $W$ ,  $\sigma^2$  and  $\mathcal{K}$  to start the procedure described in the previous Subsection. First, we notice that since equation (2), the distribution of  $\mathbf{Y}$  is a wrapped normal  $WN_D(\boldsymbol{\mu}, C)$  with  $C = WW^\top + \sigma^2 I_D$ . Using the CEM algorithm in Nodehi et al. [2020] and also Section SM-3 in the Supplementary Material and an unstructured variance and covariance matrix  $\Sigma$  instead of  $C$  we obtain (initial) estimates  $\hat{\boldsymbol{\mu}}_0$ ,  $\hat{\mathcal{K}}_0 = (\hat{\mathbf{k}}_1, \dots, \hat{\mathbf{k}}_N)$  and  $S$  as estimate of  $\boldsymbol{\mu}$ ,  $\mathcal{K}$  and  $\Sigma$  respectively, with the form

$$\hat{\boldsymbol{\mu}}_0 = \frac{1}{N} \sum_{j=1}^N (\mathbf{y}_j + 2\pi \hat{\mathbf{k}}_j)$$

and

$$S = \frac{1}{N} \sum_{j=1}^N (\mathbf{y}_j + 2\pi \hat{\mathbf{k}}_j - \hat{\boldsymbol{\mu}}_0)(\mathbf{y}_j + 2\pi \hat{\mathbf{k}}_j - \hat{\boldsymbol{\mu}}_0)^\top .$$

Turning back to the original model for  $\mathbf{Y} \sim WN_D(\boldsymbol{\mu}, C)$  and using  $\hat{\mathcal{K}}_0$  the log-likelihood function, of the remaining parameters  $\boldsymbol{\mu}$ ,  $W$ ,  $\sigma^2$ , has the form

$$\ell(\boldsymbol{\mu}, W, \sigma^2, \hat{\mathcal{K}}) \propto -N \ln(\det(C)) - \sum_{j=1}^N (\mathbf{y}_j + 2\pi \hat{\mathbf{k}}_j - \boldsymbol{\mu})^\top C^{-1} (\mathbf{y}_j + 2\pi \hat{\mathbf{k}}_j - \boldsymbol{\mu}) .$$

This log-likelihood is also maximized by  $\hat{\boldsymbol{\mu}}_0$  and by back-substituting it into the log-likelihood, we have

$$\ell(\hat{\boldsymbol{\mu}}_0, W, \sigma^2, \hat{\mathcal{K}}_0) \propto -(\ln(\det(C)) + \text{tr}(C^{-1}S)) .$$

which is the same as equation (SM–5) of Section SM–2.1 of the Supplementary Material and as expected the estimates of  $W$  and  $\sigma^2$  are the same, i.e.,

$$\hat{W}_0 = U_d(\Lambda_d - \hat{\sigma}_0^2 I_d)^{\frac{1}{2}} V_d^\top$$

where  $\Lambda_d$  and  $U_d$  are the first  $d$  principal eigenvalues and the  $d$  corresponding eigenvectors of  $S$  and

$$\hat{\sigma}_0^2 = \frac{\text{tr}(\Lambda_{D-d})}{D-d} = \frac{\sum_{i=d+1}^D \lambda_i}{D-d}$$

where  $\Lambda_{D-d}$  contains the last  $D-d$  eigenvalues of  $S$ , that is,  $\hat{\sigma}_0^2$  is the average of the discarded eigenvalues of  $S$  [Tipping and Bishop, 1999].

## 5 Selection of the number of components

One of the challenging problem in dimensional reduction problems such as PCA or Factor Analysis (FA) is how to compute the number of components. Many methods have been proposed in last decades, e.g. (a) Proportion of Variance [Jackson, 1991], (b) Kaiser-Guttman which is the number of eigenvalues of the sample correlation matrix that are greater than unity (Guttman [1954] and Kaiser [1960]), (c) the number of positive eigenvalues of the sample correlation matrix whose  $j$ th diagonal element is replaced by the squared multiple correlation between the  $j$ th variable and the rest of the  $p-1$  variables,  $j = 1, \dots, p$  [Hayashi et al., 2007], (d) the scree plot [Cattell, 1966], a visual plotting procedure to separate the largest eigenvalues of the sample correlation or covariance matrix from the smallest eigenvalues that are linearly decreasing, (e) the Likelihood Ratio Test (LRT) [Bartlett, 1950, Jöreskog, 1967] for Maximum Likelihood Factor Analysis; (f) Akaike information criterion (AIC) [Akaike, 1987] and its variants such as CAIC [Bozdogan, 1994] and BIC [Schwarz, 1978] and (g) Cross-Validation which is proposed by Krzanowski [1987] and described in SM–4 of the Supplementary Material.

As the PPCA is an extension of PCA which has a probabilistic model, we suggest to use Likelihood Ratio Test (LRT) as in Factor Analysis [Lawley and Maxwell, 1971, Bartlett, 1950].

There are two different ways to test about the number of factors using LRT, both are regularly used in covariance structure analysis. One amount to the standard model goodness-of-fit test (Type 1), whereas the other involves a chi-square difference test (Type 2). Let us start by introducing the LRT and explain how to extend it to TPPCA.

If the distribution of the random samples  $\mathcal{X} = (\mathbf{X}_1, \dots, \mathbf{X}_n)^\top$  depends upon a parameter vector  $\boldsymbol{\theta} \in \Theta$  and if  $H_0 : \boldsymbol{\theta} \in \Theta_0$  and  $H_1 : \boldsymbol{\theta} \in \Theta_1 = \Theta/\Theta_0$  are any hypotheses, then the likelihood ratio statistics for testing  $H_0$  against  $H_1$  is defined as

$$\lambda = \frac{L_0^*}{L_1^*},$$

where  $L_i^*$  is the largest value which the likelihood function takes in region  $\Theta_i$ ,  $i = 0, 1$ . Equivalently, we might use the log-likelihood statistics

$$-2 \log \lambda = -2(l_0^* - l_1^*)$$

where  $l_i^* = \log L_i^*$ ,  $i = 0, 1$  [Mardia et al., 1979].

### **Type 1: Chi-square test for testing the $d$ -component model against the saturated model**

In the first approach we consider the following system of hypothesis

$$H_0 : \Sigma = \Sigma_0$$

$$H_1 : \Sigma \text{ is any positive definite matrix}$$

where, based on equation (2),  $\Sigma_0 = WW^\top + \sigma^2 I_D$ . Thus, to perform the LRT, we have

$$\begin{aligned} l_0^* &= -\frac{n}{2} \log |2\pi \Sigma_0| - \frac{n}{2} \text{tr}(\Sigma_0^{-1} S) \\ l_1^* &= -\frac{n}{2} \log |2\pi S| - \frac{n}{2} \text{tr}(S^{-1} S), \end{aligned}$$

which in the last line  $-\frac{n}{2} \text{tr}(S^{-1}S) = -\frac{nD}{2}$ . The statistical test is given by

$$\begin{aligned}
U_d &= -2 \log \lambda = -2 \log(L_0^* - L_1^*) \\
&= -2 \left( -\frac{n}{2} \log |2\pi \Sigma_0| - \frac{n}{2} \text{tr}(\Sigma_0^{-1}S) + \frac{n}{2} \log |2\pi S| + \frac{nD}{2} \right) \\
&= n \log |\Sigma_0| + n \text{tr}(\Sigma_0^{-1}S) - n \log |S| - nD \\
&= -n \log |\Sigma_0^{-1}S| + n \text{tr}(\Sigma_0^{-1}S) - nD \\
&= -n \log (g^D) + n(Da) - nD \\
&= -nD \log g + nDa - nD \\
&= nD(a - \log g - 1) .
\end{aligned} \tag{3}$$

Note that this statistic is a function of eigenvalue of  $\Sigma_0^{-1}S$ , where we denote by  $a$  the arithmetic mean of the eigenvalues of  $\Sigma_0^{-1}S$  and by  $g$  the geometric mean, so that  $\text{tr}(\Sigma_0^{-1}S) = Da$  and  $|\Sigma_0^{-1}S| = g^D$ , then  $-2 \log \lambda = nD(a - \log g - 1)$ . Moreover, this statistic has an asymptotic  $\chi_m^2$  distribution under  $H_0$  with  $m = \frac{D(D+1)}{2} - t$  and where  $t$  is the number of free parameters in the model. More precisely, in our situation  $t = (Dd + 1 - \frac{d(d-1)}{2})$ .

## **Type 2: Chi-square difference test for testing the $d$ -component model against the $(d+1)$ -component model**

In this second approach we consider the following system of hypothesis

$$\begin{aligned}
H_0 &: \Sigma = \Sigma_0 \text{ with at most } d\text{-component} \\
H_1 &: \Sigma = \Sigma_0 \text{ with at most } (d+1)\text{-component} ,
\end{aligned}$$

it is easy to see that for this system the LRT statistic is given by

$$V_d = U_d - U_{d+1} ,$$

where  $U_d$  and  $U_{d+1}$  are computed by equation (3). In this regard,  $V_d$  is approximately distributed as a Chi-square variate with  $(D - d)$  degrees of freedom. In Factor Analysis, the Bartlett correction is usually not applied to the difference test, so we prefer to use **Type 2** in our work due to difference between Probabilistic PCA and Factor Analysis.

Again like in Factor Analysis, in either case, in the absence of a priori knowledge, a typical procedure for implementing these tests is in a forward stepwise manner. That is, we might start with a 1-component model, and



estimate it, yielding a model test for  $H_0$  with  $d = 1$  component. If  $H_0$  is rejected, we next increase  $d$  by 1 and estimate a 2-component model, testing  $H_0$  with  $d = 2$  components; if  $H_0$  is rejected again, then we proceed with  $d = 3$  components. At each step in the process, we can use either or both versions of the LRT. Subsequently, we continue this estimation and testing process until we fail to reject  $H_0$ ; at that point we take the current  $d$  as the estimated number of components.

## 6 Simulation

We illustrate the performance of the TPPCA with respect to PPCA by a Monte Carlo experiment. We consider the following factors: sample size  $n = 50, 100, 500$ , upper dimension  $D = 5$ , lower dimension  $d = 2, 3$  and  $\sigma_0 = (\pi/8, \pi/4, \pi/2, \pi, 3/2\pi, 2\pi)$ ; number of Monte Carlo replications is set to 100. Here  $d$  was kept fixed to the true value. Afterwards, we compare the two methods by (i) Mean Square Error of the reconstructed  $X$  ( $X_{recons}$ ), i.e.  $\text{MSE}(X_{recons}) = \mathbb{E}(X_{recons} - X_{orig})^2$  and (ii) Mean Absolute Error of  $X_{recons}$ , i.e.,  $\text{MAE}(X_{recons}) = \mathbb{E}|X_{recons} - X_{orig}|$ , (iii) Mean Square Error of the reconstructed latent variable  $Z$  ( $Z_{recons}$ ) and (iv) Mean Absolute Error of  $Z_{recons}$ . We summarize the results in Table 1–2. Torus PPCA always outperform PPCA. When the standard deviation is increasing, the MSE of  $X_{recons}$  for Torus PPCA is increasing, as well. Furthermore, the effect of sample size in this method makes the results more accurate. In other words, considering periodic feature of angles and extending the PPCA to TPPCA improves notably the results. Also, as lower dimension ( $d$ ) increases, these two criteria increase for both considered methods.

In real cases choosing the value of the lower dimension is necessary. With this aim we run a second Monte Carlo experiment where we choose the dimension by Cross-Validation (CV), Kaiser-Guttman and Likelihood Ratio Test (LRT) in order to estimate the number of component ( $d$ ) as explained in Section 5. Tables 3–4 report the performance of TPPCA based on the three different procedures. Very small differences, in term of the performance measures used, are observed among the three methods, with perhaps a little preference, overall, for the Likelihood Ratio Test. Full results are reported in Section SM–5 of the Supplementary Material, they show that the LRT has the overall best performance among the considered methods in estimating the dimension  $d$ .

Lower dim.	Methods	$\sigma$	MSE( $X_{recons}$ )			MAE( $X_{recons}$ )		
			$n = 50$	$n = 100$	$n = 500$	$n = 50$	$n = 100$	$n = 500$
$d = 2$	TPPCA	$\frac{\pi}{8}$	1.589	1.654	0.879	0.657	0.637	0.460
		$\frac{\pi}{4}$	2.385	2.152	1.500	0.930	0.845	0.671
		$\frac{\pi}{2}$	3.285	3.068	3.068	1.247	1.190	1.145
		$\pi$	4.230	4.305	4.159	1.581	1.582	1.529
		$\frac{3\pi}{2}$	4.498	4.634	4.606	1.663	1.684	1.676
		$2\pi$	4.950	4.960	4.901	1.747	1.756	1.752
	PPCA	$\frac{\pi}{8}$	16.430	16.324	16.519	3.294	3.289	3.297
		$\frac{\pi}{4}$	15.688	15.465	15.575	3.290	3.253	3.269
		$\frac{\pi}{2}$	14.906	14.395	14.475	3.262	3.224	3.234
		$\pi$	14.289	13.915	13.808	3.264	3.240	3.224
		$\frac{3\pi}{2}$	13.917	13.842	13.487	3.250	3.245	3.216
		$2\pi$	13.755	13.620	13.156	3.243	3.236	3.211
$d = 3$	TPPCA	$\frac{\pi}{8}$	3.738	2.868	2.397	1.152	0.953	0.788
		$\frac{\pi}{4}$	4.309	4.060	3.092	1.400	1.289	1.039
		$\frac{\pi}{2}$	5.392	5.120	4.512	1.708	1.625	1.448
		$\pi$	5.884	6.073	5.919	1.890	1.910	1.865
		$\frac{3\pi}{2}$	6.117	6.415	6.326	1.950	1.990	1.975
		$2\pi$	6.376	6.338	6.927	1.997	1.996	2.081
	PPCA	$\frac{\pi}{8}$	18.018	17.852	17.988	3.368	3.344	3.365
		$\frac{\pi}{4}$	17.257	17.459	17.260	3.345	3.368	3.339
		$\frac{\pi}{2}$	16.519	16.448	16.262	3.340	3.341	3.314
		$\pi$	16.005	15.562	15.406	3.361	3.317	3.306
		$\frac{3\pi}{2}$	15.370	15.405	15.184	3.328	3.325	3.318
		$2\pi$	15.413	15.232	15.037	3.335	3.329	3.310

Table 1: Performance of TPPCA and PPCA on the reconstruction of  $X$  measured by MSE and MAE using true value of  $d$  and  $D = 5$ .

Lower dim.	Methods	$\sigma$	MSE( $Z_{recons}$ )			MAE( $Z_{recons}$ )		
			$n = 50$	$n = 100$	$n = 500$	$n = 50$	$n = 100$	$n = 500$
$d = 2$	TPPCA	$\frac{\pi}{8}$	1.943	2.049	1.946	0.991	1.010	0.927
		$\frac{\pi}{4}$	2.460	2.355	1.952	1.197	1.134	0.980
		$\frac{\pi}{2}$	2.664	2.658	2.533	1.285	1.275	1.224
		$\pi$	2.560	2.592	2.538	1.290	1.294	1.269
		$\frac{3\pi}{2}$	2.559	2.467	2.398	1.290	1.267	1.243
		$2\pi$	2.620	2.410	2.427	1.307	1.253	1.252
	PPCA	$\frac{\pi}{8}$	9.327	9.222	9.388	2.574	2.560	2.570
		$\frac{\pi}{4}$	7.849	7.936	7.722	2.336	2.358	2.329
		$\frac{\pi}{2}$	6.753	6.659	6.425	2.159	2.136	2.108
		$\pi$	5.956	5.573	5.202	2.001	1.935	1.872
		$\frac{3\pi}{2}$	5.539	5.218	4.863	1.928	1.865	1.798
		$2\pi$	5.395	5.073	4.687	1.901	1.838	1.758
$d = 3$	TPPCA	$\frac{\pi}{8}$	2.343	2.354	2.118	1.168	1.146	1.031
		$\frac{\pi}{4}$	2.642	2.438	2.553	1.285	1.200	1.185
		$\frac{\pi}{2}$	2.579	2.721	2.696	1.280	1.308	1.278
		$\pi$	2.483	2.520	2.491	1.264	1.276	1.259
		$\frac{3\pi}{2}$	2.509	2.456	2.499	1.275	1.256	1.267
		$2\pi$	2.522	2.439	2.419	1.279	1.257	1.250
	PPCA	$\frac{\pi}{8}$	6.228	6.208	5.731	2.059	2.063	1.970
		$\frac{\pi}{4}$	5.956	5.641	5.559	2.006	1.953	1.944
		$\frac{\pi}{2}$	5.475	5.350	5.161	1.922	1.898	1.870
		$\pi$	5.190	5.008	4.792	1.857	1.827	1.787
		$\frac{3\pi}{2}$	5.021	4.877	4.637	1.829	1.796	1.748
		$2\pi$	4.949	4.754	4.553	1.817	1.776	1.731

Table 2: Performance of TPPCA and PPCA on the reconstruction of  $X$  measured by MSE and MAE using true value of  $d$  and  $D = 5$ .

Lower dim.	Method	$\sigma$	MSE( $X_{recons}$ )			MAE( $X_{recons}$ )		
			$n = 50$	$n = 100$	$n = 500$	$n = 50$	$n = 100$	$n = 500$
$d = 2$	CV	$\frac{\pi}{8}$	1.637	1.561	1.259	0.701	0.676	0.561
		$\frac{\pi}{4}$	2.527	2.347	1.769	0.977	0.897	0.754
		$\frac{\pi}{2}$	2.883	3.024	2.746	1.178	1.187	1.072
		$\pi$	3.956	3.937	3.742	1.513	1.508	1.445
		$\frac{3\pi}{2}$	4.094	4.379	4.557	1.571	1.625	1.656
		$2\pi$	4.610	4.650	4.882	1.674	1.684	1.739
	KG	$\frac{\pi}{8}$	1.745	1.531	1.115	0.719	0.625	0.510
		$\frac{\pi}{4}$	2.381	1.979	1.696	0.927	0.812	0.716
		$\frac{\pi}{2}$	3.396	3.170	2.676	1.274	1.201	1.053
		$\pi$	4.345	4.212	4.304	1.600	1.566	1.554
		$\frac{3\pi}{2}$	4.556	4.604	4.743	1.676	1.686	1.704
		$2\pi$	4.953	4.874	4.913	1.749	1.750	1.752
	LRT	$\frac{\pi}{8}$	1.736	1.450	1.009	0.692	0.605	0.470
		$\frac{\pi}{4}$	2.575	2.396	1.590	0.988	0.890	0.694
		$\frac{\pi}{2}$	2.839	2.973	2.724	1.159	1.161	1.065
		$\pi$	3.606	3.580	3.861	1.427	1.418	1.458
		$\frac{3\pi}{2}$	4.058	4.009	4.450	1.546	1.540	1.637
		$2\pi$	4.192	4.082	4.545	1.583	1.571	1.670

Table 3: Performance of TPPCA and PPCA on the reconstruction of  $X$  measured by MSE and MAE using an estimated value of  $d$  by several methods,  $D = 5$ , true value of  $d$  is 2.

Lower dim.	Method	$\sigma$	MSE( $X_{recons}$ )			MAE( $X_{recons}$ )		
			$n = 50$	$n = 100$	$n = 500$	$n = 50$	$n = 100$	$n = 500$
$d = 3$	CV	$\frac{\pi}{8}$	3.506	3.232	2.795	1.167	1.082	0.966
		$\frac{\pi}{4}$	3.810	3.632	2.985	1.307	1.234	1.049
		$\frac{\pi}{2}$	4.383	4.447	4.123	1.516	1.505	1.385
		$\pi$	5.147	5.185	4.992	1.743	1.734	1.690
		$\frac{3\pi}{2}$	5.501	5.880	5.342	1.827	1.886	1.802
		$2\pi$	5.553	5.688	5.503	1.841	1.862	1.835
	KG	$\frac{\pi}{8}$	3.509	3.029	2.642	1.164	1.023	0.903
		$\frac{\pi}{4}$	3.826	3.914	3.202	1.296	1.272	1.081
		$\frac{\pi}{2}$	4.992	4.632	4.127	1.639	1.530	1.376
		$\pi$	5.477	5.524	5.400	1.809	1.804	1.763
		$\frac{3\pi}{2}$	5.637	5.839	5.962	1.863	1.894	1.912
		$2\pi$	5.812	5.894	6.066	1.904	1.917	1.941
	LRT	$\frac{\pi}{8}$	3.539	3.007	2.467	1.165	1.013	0.819
		$\frac{\pi}{4}$	4.124	3.445	3.202	1.386	1.189	1.071
		$\frac{\pi}{2}$	4.191	4.265	4.137	1.489	1.472	1.397
		$\pi$	4.754	4.700	4.956	1.659	1.655	1.677
		$\frac{3\pi}{2}$	5.227	5.183	5.594	1.762	1.761	1.835
		$2\pi$	5.299	5.059	5.681	1.764	1.751	1.867

Table 4: Performance of TPPCA and PPCA on the reconstruction of  $X$  measured by MSE and MAE using an estimated value of  $d$  by several methods,  $D = 5$ , true value of  $d$  is 3.

## 7 Real Application: RNA data set

We consider two data sets (**small RNA** and **big RNA**) based on Ribonucleic acid (RNA) which are studied by Eltzner et al. [2018] and Nodehi et al. [2020]. These data sets has been used as benchmark by Sargsyan et al. [2012] to validate their method. In RNA data, each nucleic base corresponds to a backbone segment described by 6 dihedral angles and one angle for the base, giving a total of 7 angles. Here, we analyze small RNA and in Section SM-6 of the Supplementary Material the results for big RNA are available. The small RNA data set contains 181 observations which form three clusters in the  $\eta - \theta$  plot as shown in Figure 1. As it is shown in Figure 2 the TPPCA grouped the data in 3 clusters when the first two principal components are used, resemble the same structure as in the  $\eta - \theta$  plot, while using the two principal components from PPCA the group structure is completely lost.

## 8 Conclusions

We introduced a novel dimension reduction method based on Probabilistic PCA for data on torus. We compare its performance with Probabilistic PCA by a simulation study and we illustrate the new procedure using two RNA data sets. To determine appropriate number of components, we introduce statistical tests based on the likelihood ratio statistics.

## Acknowledgments

The authors thank Stephan Huckemann and Benjamin Eltzner for preparing RNA data set.

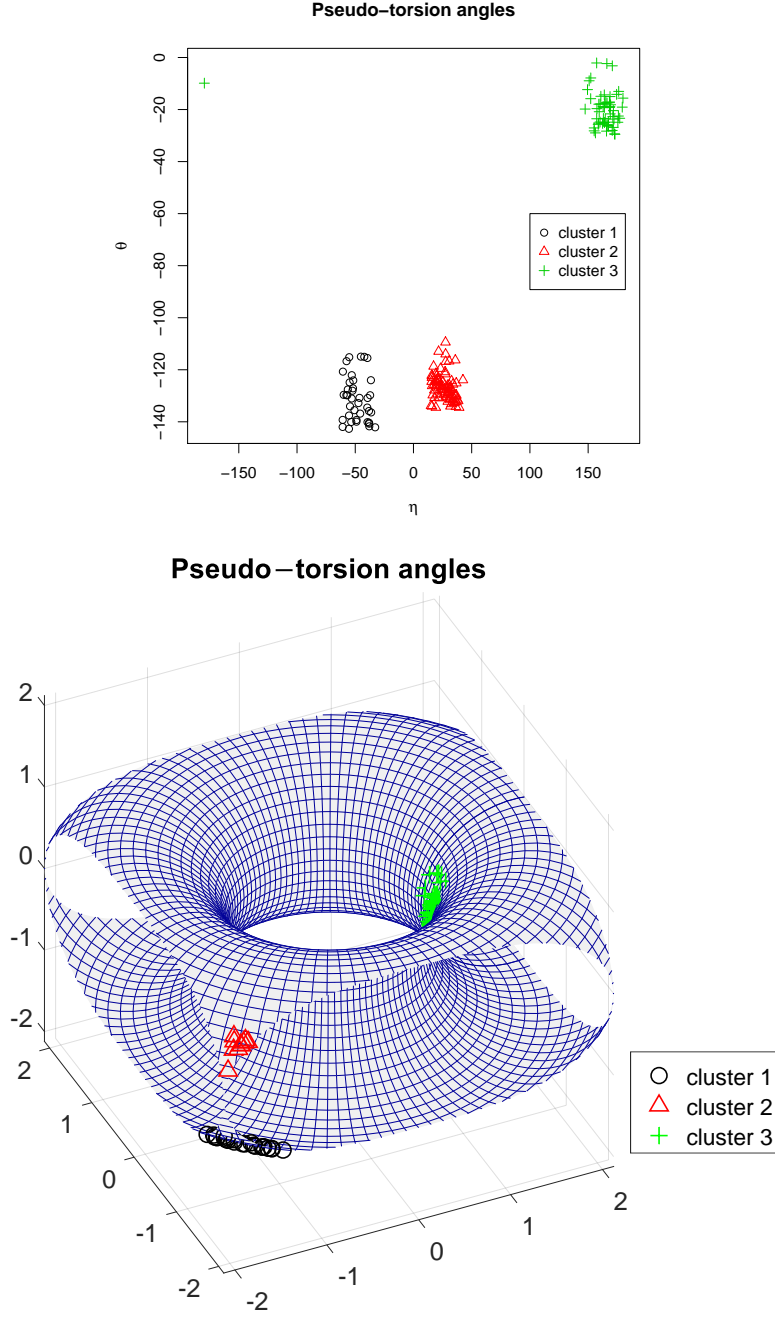


Figure 1: RNA data set. Their three preselected clusters in the  $\eta - \theta$  plot in  $2D$  (top) and on the torus (bottom).

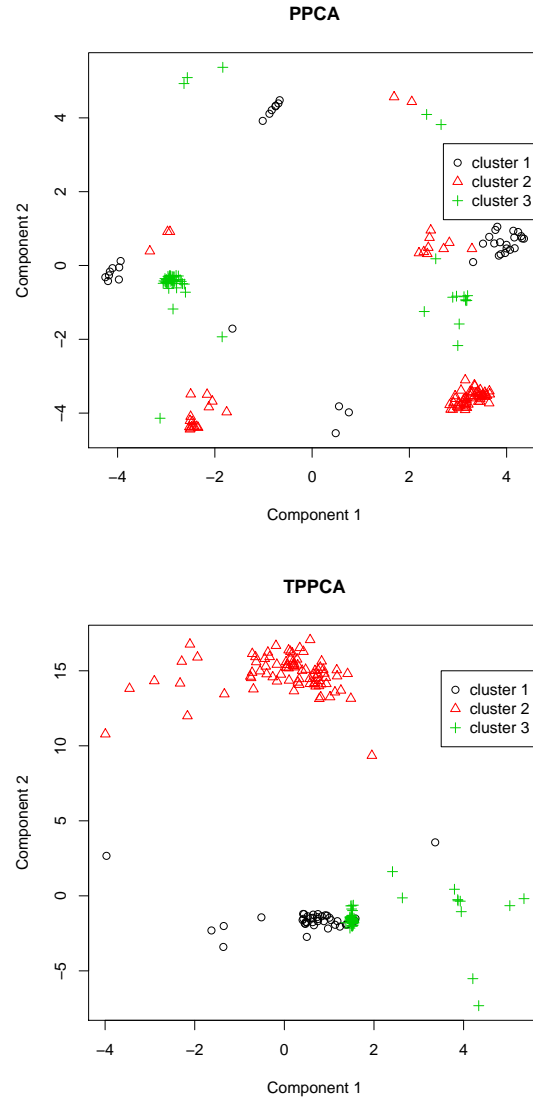


Figure 2: RNA data set. The two-dimensional representation of two first components based on PPCA (top) and TPPCA (bottom).



## Supplementary Material

The Supplementary Material contains a short review of the methods presented in literature for performing dimension reduction in non-Euclidean space (Section SM-1). Section SM-2 discusses how to estimate the parameters in PPCA model using either matrix decomposition or EM algorithm. Further, Section SM-3 reviews the estimation procedure based on Classification EM algorithm for the parameters in a multivariate wrapped normal model. Section SM-5 reports further information on the Monte Carlo experiment and Section SM-6 provides a real data set example based on an RNA data set with 23 groups on 7 variables and different sample sizes.

### SM-1 Extending PCA in non-Euclidean space

Let  $M$  be a manifold and  $x_1, x_2, \dots, x_N$  a data set lying on  $M$ . According to Karcher [1977], the mean  $\mu$  is defined as

$$\mu = \arg \min_{a \in M} \sum_{i=1}^N d(x_i, a)^2, \quad (\text{SM-4})$$

where  $d(x_i, a)$  represents the manifold distance between the  $i$ -th data point and any arbitrary point  $a$  on  $M$ . This mean is known as the *intrinsic mean*. Frechet [1948] extends this concept for a general metric space [see e.g. Karcher, 1977]. Accordingly, it is sometimes called the Frechet's mean. This quantity carries along itself the concept of the tangent space which can be helpful in some circumstances.

According to Karcher [1977], for each manifold  $M \subset \mathbb{R}^d$ , it is possible to associate a linear subspace of  $\mathbb{R}^d$  to each point  $x \in M$ . Such space is called the tangent space at  $x$ , and it is denoted by  $T_x M$ . Intuitively, it is a linear subspace that best approximates the manifold  $M$  in a neighborhood of the point  $x$ . For our case, having the intrinsic mean  $\mu$ , the  $T_\mu M$  will be the tangent space to the intrinsic mean. Luckily, if the statistical analysis cannot be invoked directly on the manifold, the tangent space in the vicinity of the intrinsic mean is a suitable place to carry out those required analyzes, albeit with losing some information.

Theoretically, each point  $x_i \in M$  can be reached by vector  $X_i \in T_\mu M$ , using the transformation  $\text{Exp}_\mu X_i = x_i$ , where  $\text{Exp}_p$  is the exponential map

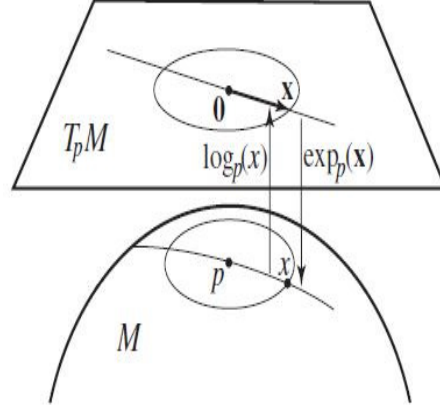


Figure SM-3: Exp map and Log map on the manifold  $M$ . This is a schematic (not exact) representation of two points lied on the two spaces.

that maps straight lines through the origin  $T_p M$  over geodesics on  $M$  passing through the point  $x \in M$ . Following Pennek (2006), the geodesic is a curve with locally shortest path between two points. Note that the inverse map for transferring  $x_i \in M$  to  $X_i \in T_\mu M$  is known as the logarithmic map and is usually denoted by  $\text{Log}_\mu x_i$ . Figure SM-3 gives a schematic representation of these maps.

Now, having a tool for connecting points on two spaces, the extension of PCA on manifold can easily be defined. They are as follows.

### SM-1.1 Principal Curve (PC)

Hastie and Stuetzle [1989] proposed the Principal Curve as an extension of PCA. In this regard, Principal Curves are smooth curves that are fit to data in Euclidean space by minimizing the sum-of-squared Euclidean distances to the data.

### SM-1.2 Principal Geodesic Analysis (PGA)

Principal Geodesic Analysis has been introduced by Fletcher et al. [2004] who used the Riemannian property of the non-Euclidean space to derive the eigenvectors and eigenvalues on the manifold through the exponential and logarithmic maps. In other words, PGA takes the tangent space of the manifold at geodesic mean as the linear space and work with appropriate mapping between the manifold and the tangent space. Elaborating on this,

it result in finding the best fitting geodesic among those passing through the geodesic mean. It is worth to note that the procedure to finding the mean is done by Gradient Descend Algorithm.

### **SM–1.3 Geodesic Principal Component Analysis (GPCA)**

Huckemann and Ziezold [2006] proposes GPCA as the extension of PCA which is for Riemannian manifolds based on geodesic of the intrinsic metric. They show the numerical implementation for data in the sphere. In that respect, they introduced a new notion of center point, the PC's mean, which is an intersection of the first two principal geodesic. This approach gives significant advantages especially when the curvature of the manifold makes the geodesic mean inadequate.

### **SM–1.4 dihedral angles Principal Component Analysis (dPCA)**

Mu et al. [2005] and Altis et al. [2007] propose dPCA as extension of PCA in torus data. To do this, a transformation from the trigonometric space of the angles to linear metric coordinate is constructed. They used this method for describing the energy landscape of small peptide in protein structure. However, the dPCA has some drawbacks, e.g., it is necessary to double the number of variables, it neglects the identity  $\cos^2 \theta + \sin^2 \theta = 1$  and it disregards the topological space of angles.

### **SM–1.5 Principal Arc Analysis (PAA)**

Jung et al. [2010] focus on direct products of simple manifolds, such as, the unit circle  $\mathbb{S}^1$ , unit sphere  $\mathbb{S}^2$ ,  $\mathbb{R}_+$  and  $\mathbb{R}^p$  (direct product manifolds). This method captures effectively more complex non-geodesic variation. For more complex direct product manifolds, they suggest transforming the data points in  $\mathbb{S}^2$  into the linear space by a special mapping by means of the principal circles. For the other components of the manifolds, the tangent mapping can be used to map the data into a linear space as done in Fletcher et al. [2004].

## SM–1.6 Principal Nested Analysis (PNS)

Jung et al. [2012] proposed a decomposition method, Principal Nested Analysis, which is a flexible extension of PCA to spheres. There has been a concern that when non-geodesic variation is major, the geodesic methods don't give a fully effective decomposition of the space. For a unit  $d$ -sphere  $\mathbb{S}^d$ , which is the set of unit vectors in  $\mathbb{R}^{d+1}$ , the analysis gives a decomposition of  $\mathbb{S}^d$  that captures the non-geodesic variation in a lower dimensional sub-sphere. The decomposition sequentially provides the best  $k$ -dimensional approximation of the data for each  $k = 0, \dots, d-1$ . The sphere  $\mathbb{S}^k$  is PNS and submanifold of higher dimensional PNS. The sequence of PNS is such that

$$\mathbb{S}^0 \subset \mathbb{S}^1 \subset \dots \subset \mathbb{S}^{d-1} \subset \mathbb{S}^d .$$

The analysis provides approximation to directional or shape data for every dimension, captures the non-geodesic variation and provides visualization of the major variability in terms of shape changes. Further, their work builds upon earlier works where PNS can be viewed as a higher dimensional extension of Principal Arc Analysis.

## SM–1.7 Principal Flows (PF)

Panaretos et al. [2014] suggested Principal Flows and demonstrate how to problem of obtaining a principal flow can be transformed into one of solving a Euler-Lagrange problem in manifold. In brief, they consider the problem of defining a smooth curve on manifold that passes through a given center of data (e.g. intrinsic mean) and with the property that, at each point, its derivative (which is tangent to the manifold) is close to the first PCA by a local tangent PCA at the same point. In this case, a flow along this curve always attempts to follow the direction of maximal variability subject to a smoothness constraint. Ultimately, they apply PF in seismological data.

## SM–1.8 dihedral angles Principal Geodesic Analysis (dPGA)

Nodehi et al. [2015] proposed the dPGA to discover the variability among dihedral angles in protein structure. The main goal of this technique is to describe the variability of a data set lying on a manifold acting through the same way as the PCA does. To do this, it is necessary to derive the

logarithmic and exponential maps in the torus. Since, there is no explicit logarithmic and exponential maps available for torus, they showed how flat torus can be approximated by the product of two circles.

## SM–2 Estimation of Parameters in PPCA model

Consider the following latent variable model that relate a  $D$ -dimensional observation vector  $\mathbf{X}$  to a corresponding  $d$ -dimensional vector of latent variables  $\mathbf{Z}$  ( $d < D$ )

$$\mathbf{X} = \boldsymbol{\mu} + W\mathbf{Z} + \boldsymbol{\epsilon}$$

where  $\mathbf{X} = (X_1, \dots, X_D)^\top$ ,  $\mathbf{Z} \sim N(\mathbf{0}, I_d)$  is an  $d$ -dimensional Gaussian latent variable, and  $\boldsymbol{\epsilon} \sim N(\mathbf{0}, \sigma^2 I_D)$  is a  $D$ -dimensional zero-mean Gaussian-distributed noise variable with covariance  $\sigma^2 I_D$ . Assume  $\text{Cov}(\mathbf{Z}, \boldsymbol{\epsilon}) = \mathbf{0}$ .

In the next subsections we are going to review two techniques based on matrix decomposition and EM algorithm in order to estimate the unknown parameters  $\boldsymbol{\mu}$ ,  $W$  and  $\sigma^2$ .

### SM–2.1 Matrix decomposition method

The log-likelihood function of the vector  $\mathbf{X} \sim N(\boldsymbol{\mu}, C)$  is given by

$$\ell(\boldsymbol{\mu}, W, \sigma^2) \propto -\frac{N}{2} \log(\det(C)) - \frac{1}{2} \sum_{j=1}^N (\mathbf{x}_j - \boldsymbol{\mu})^\top C^{-1} (\mathbf{x}_j - \boldsymbol{\mu}) ,$$

where  $C = WW^\top + \sigma^2 I_d$ . Setting the derivative of the log-likelihood with respect to  $\boldsymbol{\mu}$  equal to zero gives

$$\hat{\boldsymbol{\mu}} = \frac{1}{N} \sum_{j=1}^N \mathbf{x}_j .$$

Since the log-likelihood is a quadratic function of  $\boldsymbol{\mu}$ , this solution represents the unique maximum, as can be confirmed by computing second derivatives. Therefore, after replacing  $\hat{\boldsymbol{\mu}}$  in  $\ell$ , the log-likelihood function is on the form

$$\ell(\hat{\boldsymbol{\mu}}, W, \sigma^2) = -\frac{N}{2} \{D \log(2\pi) + \log(\det(C)) + \text{tr}(C^{-1}S)\} \quad (\text{SM-5})$$

where  $S = \sum_{j=1}^N (\mathbf{x}_j - \hat{\boldsymbol{\mu}})(\mathbf{x}_j - \hat{\boldsymbol{\mu}})^\top / N$ , is the usual sample covariance matrix. Maximization, with respect to  $W$  and  $\sigma^2$ , is more complex but nonetheless, has an exact closed-form solution. Before starting to write the derivatives, we recall that (see e.g. Vidal et al. [2016], Searle [1982] and Petersen and Pedersen [2012]) given the matrices  $A$ ,  $B$  and  $X$  with the appropriate dimension

$$\begin{aligned}\frac{\partial}{\partial X} \log(\det(X)) &= (X^{-1})^\top \\ \frac{\partial}{\partial X} \text{tr}(AX^{-1}B) &= -(X^{-1}BAX^{-1})^\top \\ \frac{\partial}{\partial X} (XBX^\top) &= XB^\top + XB.\end{aligned}$$

Thus, taking derivative of  $\ell$  with respect to  $W$  gives

$$\begin{aligned}\frac{\partial \ell}{\partial W} &= -\frac{N}{2}(C^{-1})^\top \frac{\partial C}{\partial W} - \frac{N}{2} \left( -[C^{-1}SC^{-1}]^\top \frac{\partial C}{\partial W} \right) \\ &= -\frac{N}{2}C^{-1}2W + \frac{N}{2}C^{-1}SC^{-1}2W \\ &= -NC^{-1}W + NC^{-1}SC^{-1}W,\end{aligned}$$

we recall that  $S$  and  $C$  are symmetric. Finally at stationary points, we have

$$C^{-1}W = C^{-1}SC^{-1}W. \quad (\text{SM-6})$$

There are three possible classes of solutions to (SM-6):

1.  $W = 0$  which will be seen to be a minimum of the log-likelihood.
2.  $C = S$  where the covariance model is exact and the  $D - d$  smallest eigenvalues of  $S$  are identical. Then,  $W$  is identifiable since  $WW^\top = S - \sigma^2 I_D$  has a known solution as  $W = U(\Lambda - \sigma^2 I_D)^{\frac{1}{2}}R$  where  $U$  is a square matrix whose columns are the eigenvectors of  $S$ ,  $\Lambda$  the corresponding diagonal matrix of eigenvalues, and  $R$  is an arbitrary orthogonal (i.e. rotation) matrix [Tipping and Bishop, 1997].
3. The interesting solutions represent the third case, where  $C \neq S$  and  $W \neq 0$ . To find these, we can express the parameter matrix  $W$  in terms of its Singular Value Decomposition  $W = ULV^\top$  where  $U =$

$(\mathbf{u}_1, \dots, \mathbf{u}_d)$  is a  $D \times d$  matrix of orthogonal column vectors,  $L = \text{diag}(l_1, \dots, l_d)$  is a  $d \times d$  diagonal matrix of singular values, and  $V$  is  $d \times d$  orthogonal matrix. Then, after substituting this decomposition into  $C^{-1}W$ , we have

$$\begin{aligned} C^{-1}W &= (\sigma^2 I_D + WW^\top)^{-1}W \\ &= W(\sigma^2 I_d + W^\top W)^{-1} \\ &= ULV^\top(\sigma^2 I_d + VLU^\top ULV^\top)^{-1} \\ &= ULV^\top V(\sigma^2 I_d + LU^\top UL)^{-1}V^\top \\ &= UL(\sigma^2 I_d + L^2)^{-1}V^\top, \end{aligned}$$

and after some manipulation as in (SM-6) we have

$$\begin{aligned} SUL(\sigma^2 I_d + L^2)^{-1}V^\top &= ULV^\top \\ SUL &= U(\sigma^2 I_d + L^2)L \\ SU &= U(\sigma^2 I_d + L^2), \end{aligned}$$

where  $U$  is the matrix containing the eigenvectors corresponding to eigenvalues  $(\sigma^2 I_d + L^2)$  of  $S$ . If we consider the decomposition of  $S = U\Lambda R$ , then, we are going to define

$$\begin{aligned} \Lambda_d &= (\sigma^2 I_d + L^2) \\ L^2 &= \Lambda_d - \sigma^2 I_d \\ L &= (\Lambda_d - \sigma^2 I_d)^{\frac{1}{2}}. \end{aligned}$$

So, by replacing  $L$  in  $W = ULV$  the estimation of  $W$  is given by

$$\hat{W} = U_d(\Lambda_d - \sigma^2 I_d)^{\frac{1}{2}}V_d^\top,$$

where the  $d$  column vectors in  $D \times d$  matrix  $U_d$  are the principal eigenvectors of  $S$  with corresponding eigenvalues  $\lambda_1, \dots, \lambda_d$  in the  $d \times d$  diagonal matrix  $\Lambda_d$  and  $V$  is the orthogonal rotation matrix.

Furthermore, Tipping and Bishop [1999] showed that the maximum of the likelihood function is obtained when the  $d$  eigenvectors are chosen to be those whose eigenvalues are the  $d$  largest (all other solutions being saddle points).

To back-substituting  $\hat{W}$  in equation (SM-5), we can then write

$$\begin{aligned}
\det(C) &= \det(\hat{W}\hat{W}^\top + \sigma^2 I_D) \\
&= \det(U_d(\Lambda_d - \sigma^2 I_d)U_d^\top + \sigma^2(U_d U_d^\top + U_{D-d} U_{D-d}^\top)) \\
&= \det(U_d \Lambda_d U_d^\top + \sigma^2 U_{D-d} U_{D-d}^\top) \\
&= \det \left( \begin{bmatrix} U_d & U_{D-d} \end{bmatrix} \text{diag}(\Lambda_d, \sigma^2 I_{D-d}) \begin{bmatrix} U_d^\top \\ U_{D-d}^\top \end{bmatrix} \right) \\
&= \det \left( \begin{bmatrix} \Lambda_d & 0 \\ 0 & \sigma^2 I_{D-d} \end{bmatrix} \right) \\
&= \sigma^{2(D-d)} \det(\Lambda_d) ,
\end{aligned}$$

and

$$\begin{aligned}
\text{tr}(C^{-1}S) &= \text{tr} \left[ ((U_d \Lambda_d U_d^\top + \sigma^2 U_{D-d} U_{D-d}^\top)^{-1}) (U_d \Lambda_d U_d^\top + U_{D-d} \Lambda_{D-d} U_{D-d}^\top) \right] \\
&= \text{tr} \left[ (U_d \Lambda_d^{-1} U_d^\top + \sigma^{-2} U_{D-d} U_{D-d}^\top) (U_d \Lambda_d U_d^\top + U_{D-d} \Lambda_{D-d} U_{D-d}^\top) \right] \\
&= \text{tr} \left[ U_d \Lambda_d^{-1} U_d^\top U_d \Lambda_d U_d^\top + U_d \Lambda_d^{-1} U_d^\top U_{D-d} \Lambda_{D-d} U_{D-d}^\top \right. \\
&\quad \left. + \sigma^{-2} U_{D-d} U_{D-d}^\top U_d \Lambda_d U_d^\top + \sigma^{-2} U_{D-d} U_{D-d}^\top U_{D-d} \Lambda_{D-d} U_{D-d}^\top \right] \\
&= \text{tr} \left[ U_d U_d^\top + \sigma^{-2} U_{D-d} \Lambda_{D-d} U_{D-d}^\top \right] \\
&= d + \sigma^{-2} \text{tr}(\Lambda_{D-d}) ,
\end{aligned}$$

where  $U_d U_d^\top = I_d$ ,  $U_{D-d} U_{D-d}^\top = I_{D-d}$  and  $U_{D-d}^\top U_d = U_d^\top U_{D-d} = 0$ . Recall that, given matrices  $A$  and  $B$  of appropriate dimension if  $AB^{-1}A = BA^{-1}B$ , then  $(A+B)^{-1} = A^{-1} + B^{-1}$  [Searle, 1982].

By replacing  $\det(C)$  and  $\text{tr}(C^{-1}S)$  in equation (SM-5), we can see that

$$\ell(\hat{\boldsymbol{\mu}}, \hat{W}, \sigma^2) \propto -\frac{N}{2} \left[ \log(\det(\Lambda_{D-d})) + (D-d) \log \sigma^2 + d + \sigma^{-2} \text{tr}(\Lambda_{D-d}) \right] .$$

Now by taking derivative with respect to  $\sigma^2$  we have

$$\frac{\partial \ell(\hat{\boldsymbol{\mu}}, \hat{W}, \sigma^2)}{\partial \sigma^2} = -\frac{N}{2} \left[ \frac{D-d}{\sigma^2} - \frac{\text{tr}(\Lambda_{D-d})}{\sigma^4} \right] ,$$

and equating it to zero, by solving for  $\sigma^2$  we have

$$\hat{\sigma}^2 = \frac{\text{tr}(\Lambda_{D-d})}{D-d} = \frac{\sum_{i=d+1}^D \lambda_i}{D-d} ,$$

which is the average of the discarded eigenvalues of  $S$  [Tipping and Bishop, 1999].



## SM-2.2 Expectation Maximization method for PPCA

The probabilistic PCA model can be expressed in terms of a marginalization over a continuous latent space in which for each data point  $\mathbf{x}_j$ , there is a corresponding latent variable  $\mathbf{z}_j$  ( $j = 1, \dots, N$ ). Hereafter we illustrate how the EM algorithm can be used to find maximum likelihood estimates of the model parameters. We notice that the conditional distributions are given by

$$\mathbf{X}|\mathbf{Z} \sim N_D(W\mathbf{Z} + \boldsymbol{\mu}, \sigma^2 I_D) \quad (\text{SM-7})$$

$$\mathbf{Z}|\mathbf{X} \sim N_d(M^{-1}W^\top(\mathbf{X} - \boldsymbol{\mu}), \sigma^2 M^{-1}) \quad (\text{SM-8})$$

where  $M = W^\top W + \sigma^2 I_d$ . Then, we compute the complete-data log-likelihood and take its expectation with respect to the posterior distribution of the latent variables evaluated using previous parameter values. Maximization of this expected complete data log-likelihood yields to new parameter values. The procedure is as follows:

$$\begin{aligned} f(\mathbf{x}, \mathbf{z}) &= f(\mathbf{x}|\mathbf{z}) \times f(\mathbf{z}) \\ &\propto (\sigma^2)^{-\frac{D}{2}} \exp \left[ -(\mathbf{x} - W\mathbf{z} - \boldsymbol{\mu})^\top (\mathbf{x} - W\mathbf{z} - \boldsymbol{\mu}) / (2\sigma^2) \right] \\ &\quad \times \exp \left\{ -\frac{\mathbf{z}^\top \mathbf{z}}{2} \right\}. \end{aligned}$$

Therefore, the log-likelihood function is

$$\begin{aligned} \ell(\boldsymbol{\mu}, W, \sigma^2) &= \ln f(\mathbf{x}, \mathbf{z}) \\ &\propto - \sum_{j=1}^N \left[ \frac{D}{2} \ln \sigma^2 + \frac{\text{tr}(\mathbf{x}_j - W\mathbf{z}_j - \boldsymbol{\mu})^\top (\mathbf{x}_j - W\mathbf{z}_j - \boldsymbol{\mu})}{2\sigma^2} + \frac{\text{tr}(\mathbf{z}_j^\top \mathbf{z}_j)}{2} \right] \\ &\propto - \sum_{j=1}^N \left[ \frac{D}{2} \ln \sigma^2 + \frac{\text{tr}(\mathbf{x}_j - \boldsymbol{\mu})(\mathbf{x}_j - \boldsymbol{\mu})^\top}{2\sigma^2} - \frac{(\mathbf{x}_j - \boldsymbol{\mu})\mathbf{z}_j^\top W^\top}{\sigma^2} \right. \\ &\quad \left. + \frac{\text{tr}(W\mathbf{z}_j\mathbf{z}_j^\top W^\top)}{2\sigma^2} + \frac{\text{tr}(\mathbf{z}_j^\top \mathbf{z}_j)}{2} \right]. \end{aligned}$$

E-Step: Take the expectation with respect to the posterior distribution over the

latent variables

$$\begin{aligned} \sum_{j=1}^N \mathbb{E}(\ell | \mathbf{X}_j = \mathbf{x}_j) \propto & - \sum_{j=1}^N \left[ \frac{D}{2} \ln \sigma^2 + \frac{\text{tr}(\mathbf{x}_j - \boldsymbol{\mu})(\mathbf{x}_j - \boldsymbol{\mu})^\top}{2\sigma^2} \right. \\ & \left. - \frac{(\mathbf{x}_j - \boldsymbol{\mu}) \mathbb{E}(\mathbf{Z}_j^\top | \mathbf{x}_j) W^\top}{\sigma^2} + \frac{\text{tr}(W \mathbb{E}(\mathbf{Z}_j \mathbf{Z}_j^\top | \mathbf{x}_j) W^\top)}{2\sigma^2} + \frac{\text{tr}(\mathbb{E}(\mathbf{Z}_j^\top \mathbf{Z}_j) | \mathbf{x}_j)}{2} \right] \end{aligned}$$

M-Step: Maximize with respect to the parameters

$$\sum_{j=1}^N \frac{\partial \mathbb{E}(\ell | \mathbf{X}_j = \mathbf{x}_j)}{\partial W} = - \sum_{j=1}^N \frac{(\mathbf{x}_j - \boldsymbol{\mu}) \mathbb{E}(\mathbf{Z}_j^\top | \mathbf{x}_j)}{\sigma^2} - \frac{1}{\sigma^2} W \mathbb{E}(\mathbf{Z}_j \mathbf{Z}_j^\top | \mathbf{x}_j)$$

and by equating it to 0 we have

$$\tilde{W} = \left[ \sum_{j=1}^N (\mathbf{x}_j - \boldsymbol{\mu}) \mathbb{E}(\mathbf{Z}_j^\top | \mathbf{x}_j) \right] \left[ \sum_{j=1}^N \mathbb{E}(\mathbf{Z}_j \mathbf{Z}_j^\top | \mathbf{x}_j) \right]^{-1}.$$

and, in a similar way

$$\begin{aligned} \sum_{j=1}^N \frac{\partial \mathbb{E}(\ell | \mathbf{X}_j = \mathbf{x}_j)}{\partial \sigma^2} = & - \sum_{j=1}^N \left[ \frac{D}{2\sigma^2} - \frac{1}{2\sigma^4} [(\mathbf{x}_j - \boldsymbol{\mu})(\mathbf{x}_j - \boldsymbol{\mu})^\top - 2(\mathbf{x}_j - \boldsymbol{\mu}) \mathbb{E}(\mathbf{Z}_j^\top | \mathbf{x}_j) W^\top \right. \\ & \left. + \text{tr}(W \mathbb{E}(\mathbf{Z}_j \mathbf{Z}_j^\top | \mathbf{x}_j) W^\top)] \right] = 0 \end{aligned}$$

which leads to the estimates

$$\begin{aligned} \tilde{\sigma}^2 = & \frac{1}{ND} \sum_{j=1}^N [\text{tr}(\mathbf{x}_j - \boldsymbol{\mu})(\mathbf{x}_j - \boldsymbol{\mu})^\top - 2(\mathbf{x}_j - \boldsymbol{\mu}) \mathbb{E}(\mathbf{Z}_j^\top | \mathbf{x}_j) W^\top \\ & + \text{tr}(W \mathbb{E}(\mathbf{Z}_j \mathbf{Z}_j^\top | \mathbf{x}_j) W^\top)] . \end{aligned}$$

By substituting (SM-7) in  $\tilde{W}$  and  $\tilde{\sigma}^2$ , we can see

$$\begin{aligned} \tilde{W} = & \left[ \sum_{j=1}^N \text{tr}(\mathbf{x}_j - \boldsymbol{\mu})(\mathbf{x}_j - \boldsymbol{\mu})^\top W M^{-1} \right] [N(\sigma^2 I_d - M^{-1} W^\top S W) M^{-1}]^{-1} \\ = & N S W M^{-1} M (\sigma^2 I_d - M^{-1} W^\top S W)^{-1} N^{-1} \\ = & S W (\sigma^2 I_d - M^{-1} W^\top S W)^{-1} . \end{aligned}$$

and

$$\tilde{\sigma}^2 = \frac{1}{D} \text{tr}(S - S W M^{-1} \tilde{W}^\top)$$

### SM–3 Classification EM algorithm for multivariate wrapped normal models

Here we review the CEM algorithm proposed in Nodehi et al. [2020] for estimating parameters in the following model

$$\begin{aligned} \mathbf{Y} &= \mathbf{X} \bmod 2\pi \\ \mathbf{X} &\sim N_D(\boldsymbol{\mu}, \Sigma) . \end{aligned}$$

The Classification EM (CEM) algorithm [Celeux and Govaert, 1992] is such that after the E-step it is performed a C-step (Classification step). In our context this reduces the log-likelihood to the following “classification” log-likelihood

$$\ell(\boldsymbol{\mu}, \Sigma, \mathcal{K}|\mathcal{Y}) = \sum_{j=1}^N \ln \phi(\mathbf{y}_j + 2\pi \mathbf{k}_j | \boldsymbol{\mu}, \Sigma) . \quad (\text{SM-9})$$

in which the  $\mathbf{k}_j \in \mathbb{Z}^D$  ( $j = 1, \dots, N$ ) are treated as unknown parameters and  $\phi(\cdot | \boldsymbol{\mu}, \Sigma)$  is the multivariate normal density. In this regard, the procedure is as follows

- **E-step:** Compute weights  $v_{j\mathbf{k}_j}$  as

$$v_{j\mathbf{k}_j} = \frac{\phi(\mathbf{y}_j + 2\pi \mathbf{k}_j | \boldsymbol{\mu}, \Sigma)}{\sum_{\mathbf{k}_j \in \mathbb{Z}^D} \phi(\mathbf{y}_j + 2\pi \mathbf{k}_j | \boldsymbol{\mu}, \Sigma)} , \quad \mathbf{k}_j \in \mathbb{Z}^D \quad j = 1, \dots, N ;$$

- **C-step:** Let  $\hat{\mathbf{k}}_j = \arg \max_{\mathbf{k}_j \in \mathbb{Z}^D} v_{j\mathbf{k}_j}$ ;
- **M-step:** Compute the updated estimates of  $\boldsymbol{\mu}$  and  $\Sigma$  by maximizing the classification log-likelihood conditionally on  $\hat{\mathbf{k}}_j$  ( $j = 1, \dots, N$ ).

Full details are available in Nodehi et al. [2020].

### SM–4 Number of Components: Cross-Validation

As mentioned in Section 5, one of the difficulties in PCA is how to determine the optimal number of components. In this section, we would like to explain how to use Cross-Validation procedure for choosing optimal number of components.

Suppose that, there are  $p$  variables  $X_1, \dots, X_p$  which are displayed in an  $(n \times p)$  data matrix  $X$ . Further, we assume that  $X$  has been mean-centered. Based on Singular Value Decomposition (SVD) of  $X$ , one can write

$$X = UDV^\top \quad (\text{SM-10})$$

where  $U^\top U = I_p$ ,  $V^\top V = VV^\top = I_p$  and  $D = (d_1, \dots, d_p)$  with  $d_1 \geq \dots \geq d_p \geq 0$ . If  $X$  has rank  $p$  and all the  $d_i$  ( $i = 1, \dots, p$ ) are distinct, then decomposition (SM-10) is unique apart from corresponding sign changes in  $U$  and  $V$ . If we consider  $x_{ij}$  and  $u_{ij}$  as the  $(i, j)$ -th elements of the matrices  $X$  and  $U$ , respectively, decomposition (SM-10) has its elementwise representation as

$$x_{ij} = \sum_{t=1}^p u_{it} d_t v_{tj}.$$

Thus, based on dimension reduction goal of PCA, if we consider lower dimension as  $m$ -dimensional, then the variation in the remaining  $(p-m)$  dimensions can be treated as random noise and we can postulate the  $m$ -component data as

$$x_{ij} = \sum_{t=1}^m u_{it} d_t v_{tj} + \epsilon_{ij}.$$

where  $\epsilon_{ij}$  is a residual term.

To do Cross-Validation, at first, by denoting  $X_{-j}$  as the result of deleting the  $j$ -th column and  $X_{-i}$  as the result of deleting the  $i$ -th row of  $X$ , there are the following equations:

$$X_{-i} = \bar{U} \bar{D} \bar{V}^\top$$

where  $\bar{U} = \bar{u}_{st}$ ,  $\bar{V} = \bar{v}_{st}$  and  $\bar{D} = \text{diag}(\bar{d}_1, \dots, \bar{d}_p)$  and

$$X_{-j} = \tilde{U} \tilde{D} \tilde{V}^\top$$

with  $\tilde{U} = \tilde{u}_{st}$ ,  $\tilde{V} = \tilde{v}_{st}$  and  $\tilde{D} = \text{diag}(\tilde{d}_1, \dots, \tilde{d}_{p-1})$ . After that, the predictor can be computed as

$$\hat{x}_{ij}(m) = \sum_{t=1}^m (\tilde{u}_{it} \sqrt{\tilde{d}_t}) (\bar{u}_{tj} \sqrt{\bar{d}_t}). \quad (\text{SM-11})$$

Each element on the right-hand side of this equation is obtained from the Singular Value Decomposition of  $X$  after omitting either the  $i$ -th row or the

$j$ -th column. Furthermore, the algorithms of Bunch and Nielsen [1978] and Bunch et al. [1978] compute  $\tilde{U}$ ,  $\tilde{V}$ ,  $\bar{U}$  and  $\bar{V}$  as needed in (SM-11) in a very efficient way.

Finally, according to  $\hat{x}_{ij}(m)$  for a given number  $m$  of components, the average squared discrepancy between actual and predicted values is given by

$$PRESS(m) = \frac{1}{np} \sum_{i=1}^n \sum_{j=1}^p (\hat{x}_{ij}(m) - x_{ij})^2.$$

Consider fitting components sequentially in (SM-11). Define

$$W_m = \frac{PRESS(m-1) - PRESS(m)}{D_m} \div \frac{PRESS(m)}{D_r}$$

where  $D_m$  is the number of degrees of freedom required to fit the  $m$ -th component and  $D_r$  is the number of degrees of freedom remaining after fitting the  $m$ -th component. By Considering the number of parameters to be estimated as well as all the constraints on the eigenvectors at each stage, one can show  $D_m = n + p - 2m$ . Accordingly,  $D_r$  can be obtained by successive subtraction, given  $(n-1)p$  degrees of freedom in the mean-centered matrix  $X$  [Wold, 1978]. Based on Krzanowski [1983], it is suggested that the optimal number of components is the highest value of  $m$  for which  $W_m$  is greater than 0.9.

## SM-5 Monte Carlo experiment

Figures SM-4–SM-6 and figures SM-7–SM-9 reports the frequencies of selection of dimension when the true dimension is  $d = 2$  and  $d = 3$  respectively. Each figure corresponds to a different sample size  $n = 50, 100, 500$  and each panel to a different value of  $\sigma$ .

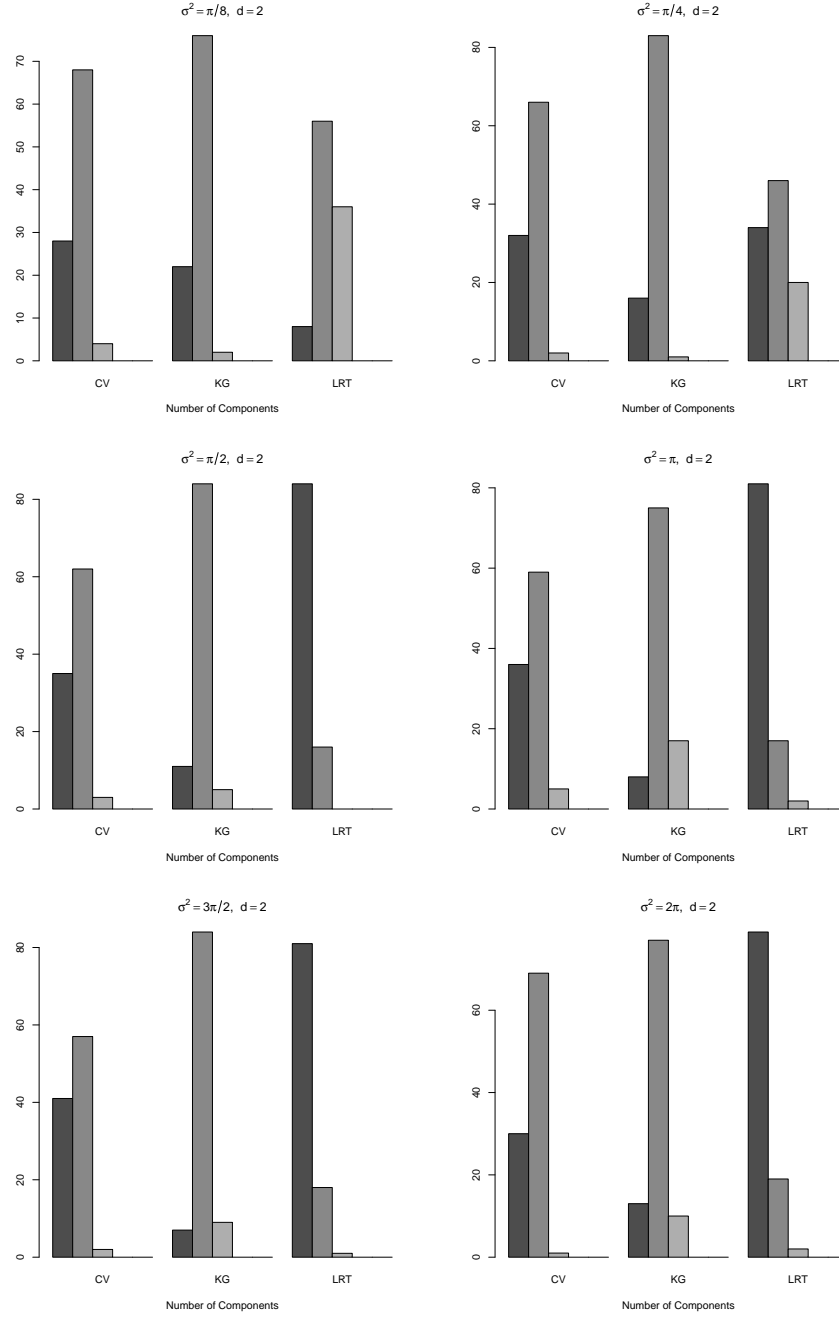


Figure SM-4: Monte Carlo experiment. Frequencies of selection of dimension for CV, KG and LRT. True value is  $d = 2$ , sample size is 50.

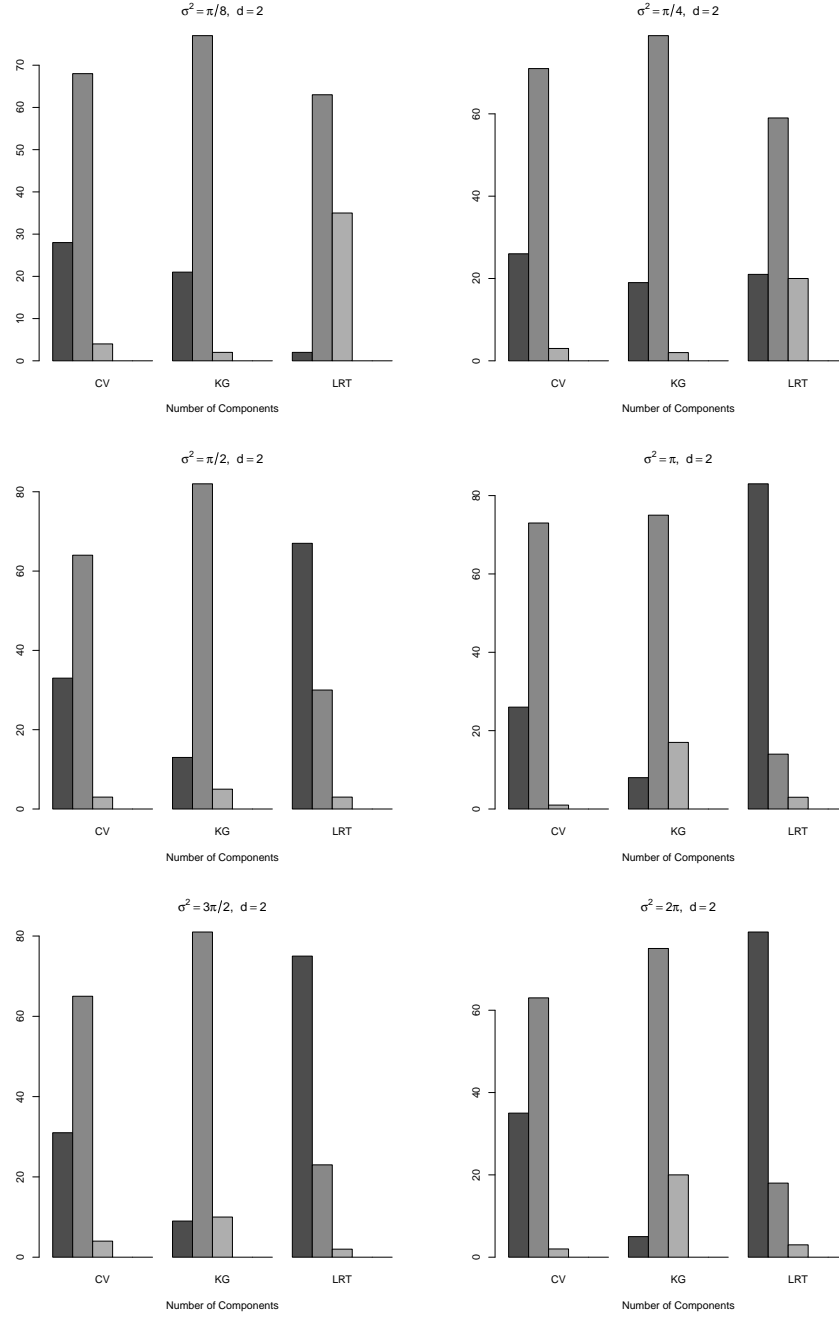


Figure SM-5: Monte Carlo experiment. Frequencies of selection of dimension for CV, KG and LRT. True value is  $d = 2$ , sample size is 100.

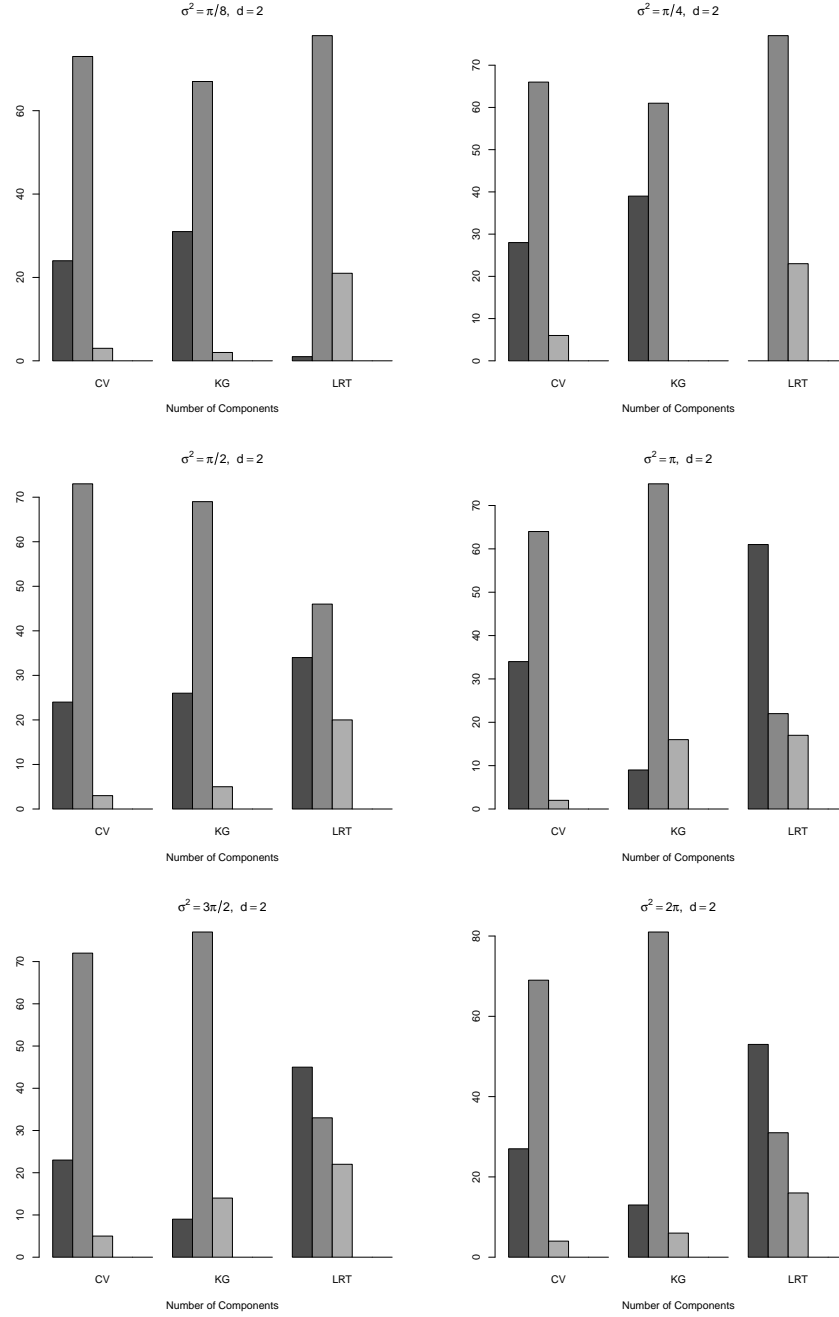


Figure SM-6: Monte Carlo experiment. Frequencies of selection of dimension for CV, KG and LRT. True value is  $d = 2$ , sample size is 500.



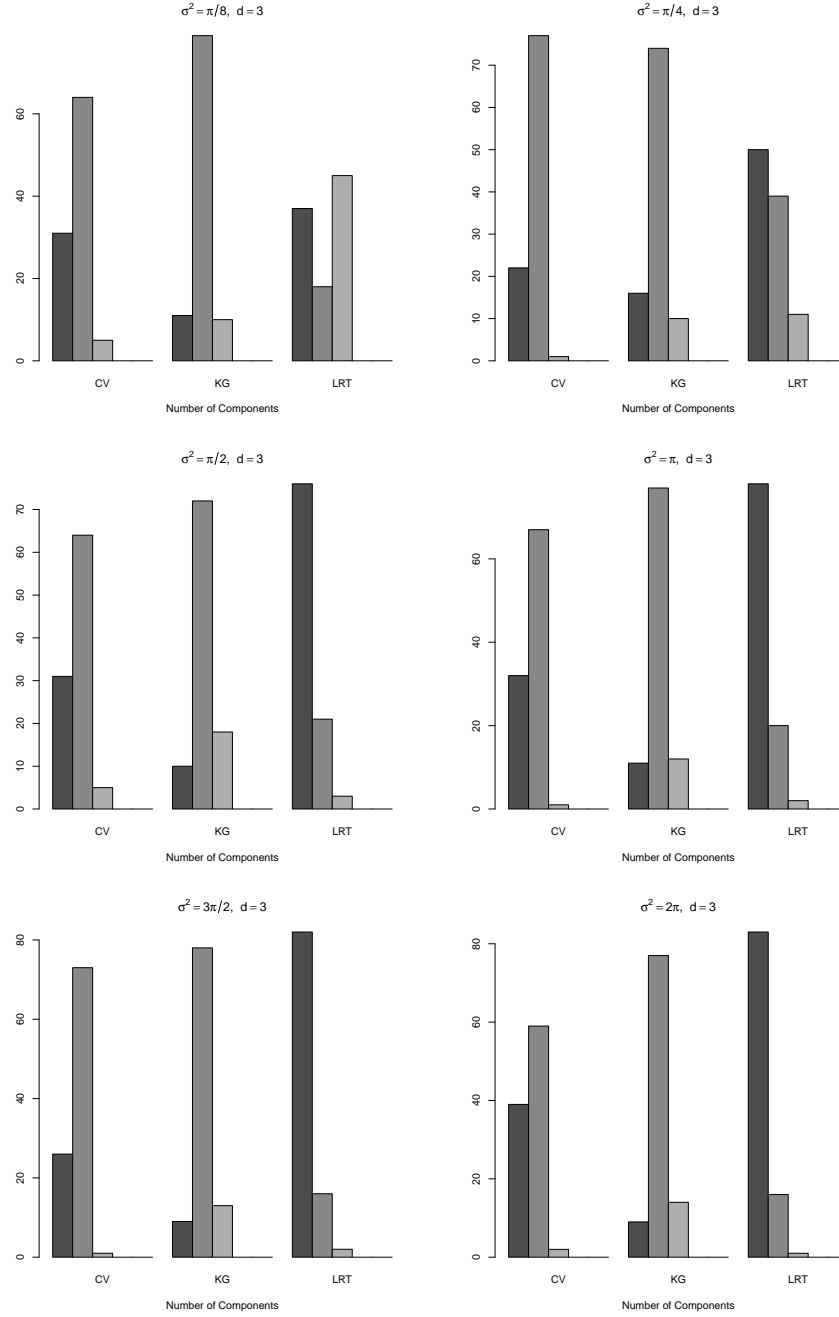


Figure SM-7: Monte Carlo experiment. Frequencies of selection of dimension for CV, KG and LRT. True value is  $d = 3$ , sample size is 50.

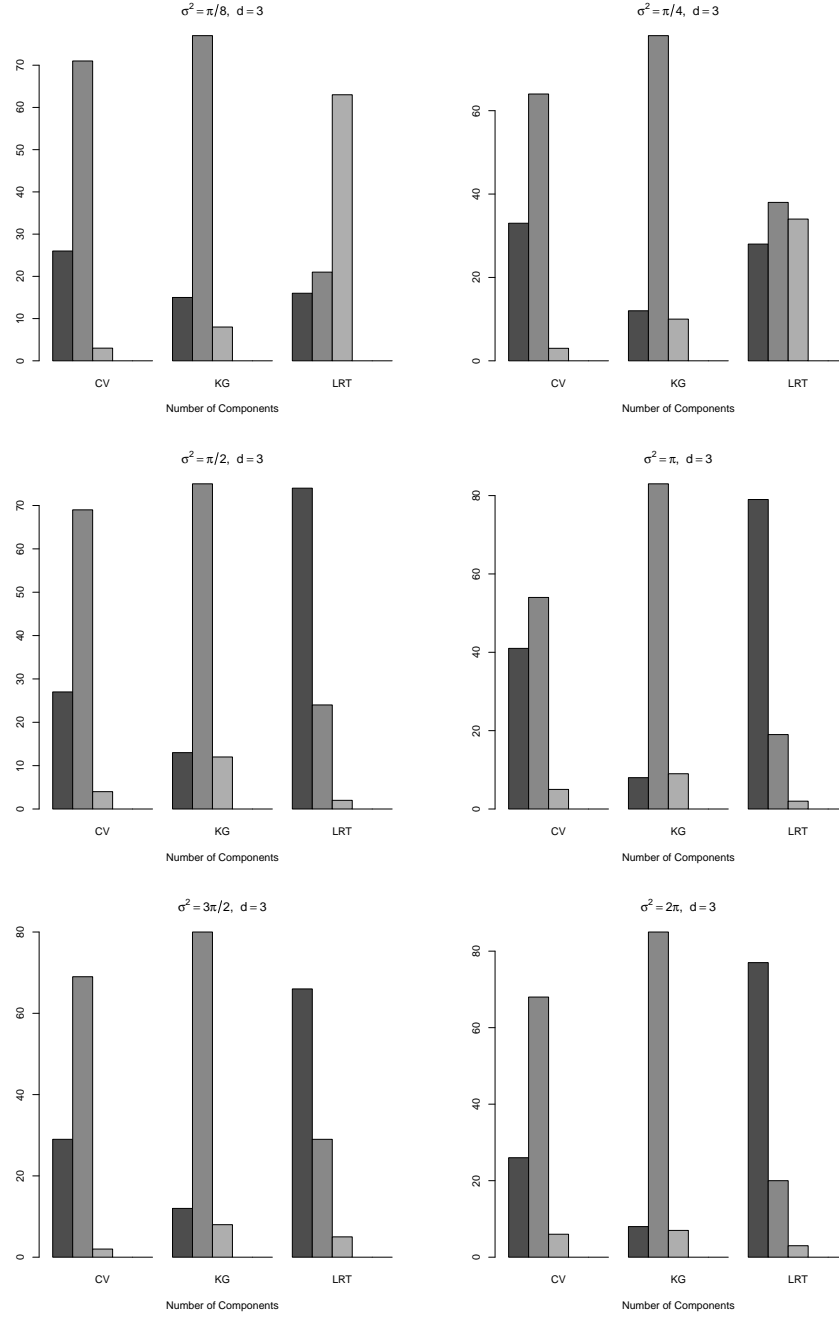


Figure SM-8: Monte Carlo experiment. Frequencies of selection of dimension for CV, KG and LRT. True value is  $d = 3$ , sample size is 100.

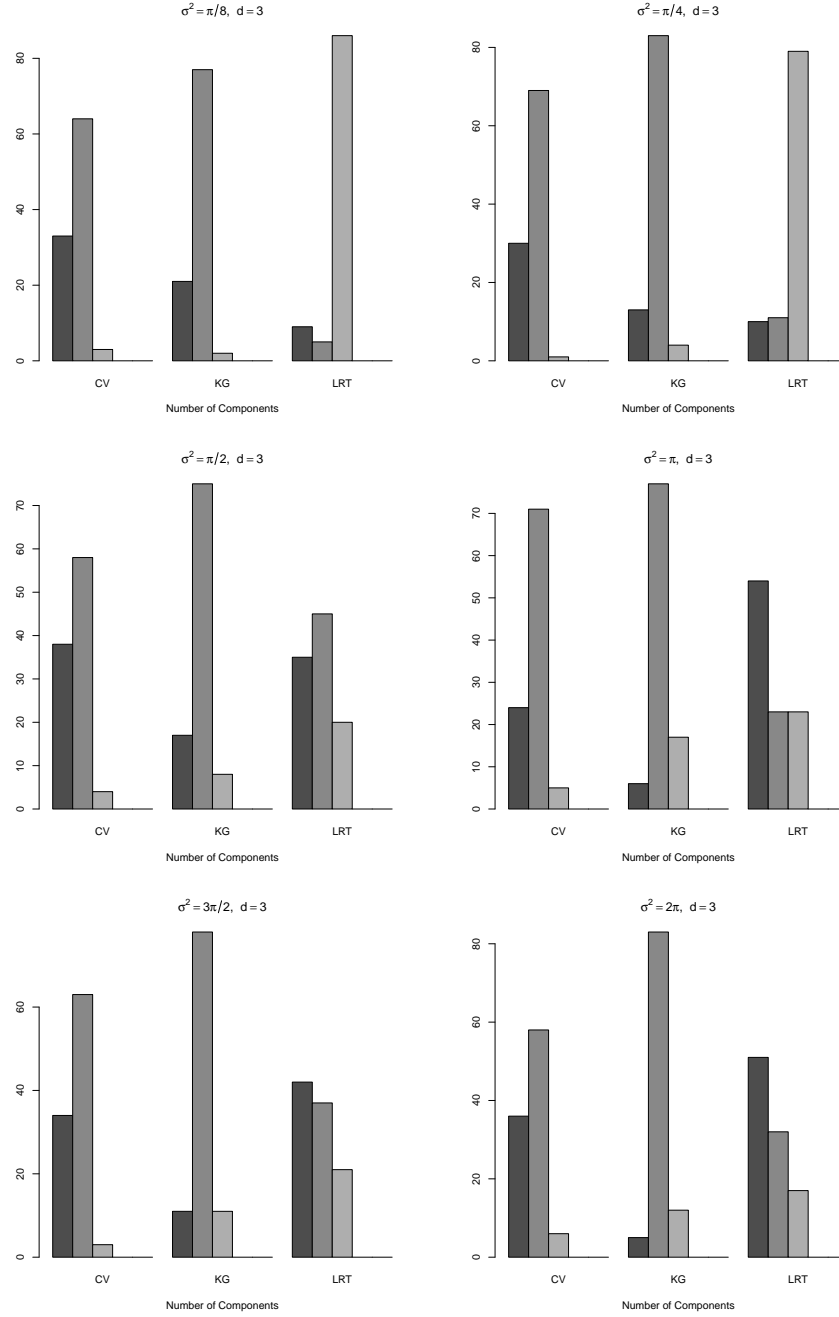


Figure SM–9: Monte Carlo experiment. Frequencies of selection of dimension for CV, KG and LRT. True value is  $d = 3$ , sample size is 500.

## SM-6 Large RNA data set

To examine the performance of TPPCA method in real application, we consider the data which are studied in Eltzner et al. [2018] and Nodehi et al. [2020]. In this data, each nucleic base corresponds to a backbone segment described by 6 dihedral angles and one angle for the base, giving a total of 7 angles. The original data set contains 8301 observations, but based on a clustering procedure the data set was split in 23 clusters and all the observations with more than  $50^\circ$  in angular distance from their nearest neighbor removed. Above that, the final data set contains 7390 observations grouped in 23 clusters. To compare the performance of our method with Probabilistic PCA, we apply both procedures in this example. As a preliminary analysis, we applied the EM and CEM algorithms in each of these clusters to estimate the mean vector and the variance and covariance matrix structure and to check the homogeneity of the groups [Nodehi et al., 2020]. In Tables SM-5 and SM-6 we reported estimated mean angles for each of the 23 clusters based on EM and CEM algorithm respectively. In addition, Figures SM-10 – SM-15 show correlation matrix by ellipses in each clusters with both the EM and CEM algorithms. Furthermore, Figures SM-16 – SM-18 report the behavior of the residual standard deviation as function the number of components for the 23 clusters.

Finally, Table SM-7 reports the performance of the three criterion (CV, KG and LRT) on the selection of number of components for each of the 23 clusters. As it is shown in Figures SM-10 – SM-15, based on both algorithms EM and CEM, in clusters 16 and 20 there are a strong correlation among some variables. For these two clusters in Figure SM-19 we show the first two principal scores which highlights inhomogeneity with the presence of subgroups.

Cluster #	# points	$\alpha$	$\beta$	$\gamma$	$\delta$	$\epsilon$	$\zeta$	$\chi$
1	4917	294.51	174.32	53.19	81.69	209.43	289.06	198.49
2	477	147.87	201.64	176.65	83.95	226.05	283.47	184.08
3	232	293.02	172.99	56.25	83.96	215.97	274.98	206.45
4	211	180.71	169.80	55.33	84.15	217.79	289.43	193.96
5	140	294.18	172.25	54.90	84.30	209.35	69.46	208.24
6	139	76.10	166.62	54.35	84.81	217.13	278.62	190.86
7	139	301.69	184.05	56.40	142.32	231.30	173.97	249.90
8	138	295.20	175.25	53.05	83.11	226.93	204.82	205.91
9	128	296.46	184.39	50.28	144.61	259.61	97.66	238.22
10	122	221.60	122.08	159.52	84.57	223.97	286.50	182.48
11	85	298.45	324.62	56.75	142.77	112.56	282.31	243.48
12	84	149.85	215.57	171.33	90.85	247.94	227.26	194.70
13	79	83.66	188.06	183.44	84.66	118.97	290.87	298.57
14	72	75.80	190.03	57.96	146.31	260.59	278.93	240.86
15	60	163.88	164.96	53.56	146.89	259.73	124.57	226.98
16	60	260.44	9.37	0.24	102.52	47.76	248.09	359.36
17	59	66.27	165.89	52.84	123.51	231.12	98.14	230.68
18	54	53.53	184.76	287.72	93.89	206.73	302.20	200.95
19	52	290.98	176.79	56.04	93.08	27.33	113.56	219.95
20	46	320.36	208.45	62.14	102.25	296.90	188.88	286.98
21	35	176.22	163.80	53.25	141.37	263.44	277.16	234.71
22	33	266.28	233.51	282.95	87.91	203.45	293.86	194.22
23	28	293.77	194.83	51.96	90.17	79.14	284.70	235.88

Table SM-5: Estimated mean of each of the 23 clusters by EM algorithm.

Cluster #	# points	$\alpha$	$\beta$	$\gamma$	$\delta$	$\epsilon$	$\zeta$	$\chi$
1	4917	294.51	174.32	53.19	81.69	209.43	289.06	198.49
2	477	147.87	201.64	176.65	83.95	226.05	283.47	184.08
3	232	293.02	172.99	56.25	83.96	215.97	274.98	206.45
4	211	180.71	169.80	55.33	84.15	217.79	289.43	193.96
5	140	294.18	172.25	54.90	84.30	209.35	69.46	208.24
6	139	76.10	166.62	54.35	84.81	217.13	278.62	190.86
7	139	301.69	184.05	56.40	142.32	231.30	173.97	249.90
8	138	295.20	175.25	53.05	83.11	226.93	204.82	205.91
9	128	296.46	184.39	50.28	144.61	259.61	97.66	238.22
10	122	221.60	122.08	159.52	84.57	223.97	286.50	182.48
11	85	298.45	180.42	56.75	142.77	256.77	282.31	243.48
12	84	149.85	215.57	171.33	90.85	247.94	226.92	194.70
13	79	83.66	188.06	183.44	84.66	220.79	290.87	196.75
14	72	75.80	190.03	57.96	146.31	260.59	278.93	240.86
15	60	163.88	164.96	53.56	146.89	259.73	124.57	226.98
16	60	272.41	15.36	354.25	102.52	53.74	248.09	353.37
17	59	66.27	165.89	52.84	123.51	231.12	98.14	230.68
18	54	53.53	184.76	287.72	93.89	206.73	302.20	200.95
19	52	290.98	176.79	56.04	93.08	27.33	113.56	219.95
20	46	337.29	208.45	62.14	102.25	313.83	171.95	303.91
21	35	176.22	163.80	53.25	141.37	263.44	277.16	234.71
22	33	266.28	233.51	282.95	87.91	203.45	293.86	194.22
23	28	293.77	194.83	51.96	90.17	79.14	284.70	235.88

Table SM-6: Estimated mean of each of the 23 clusters by CEM algorithm.

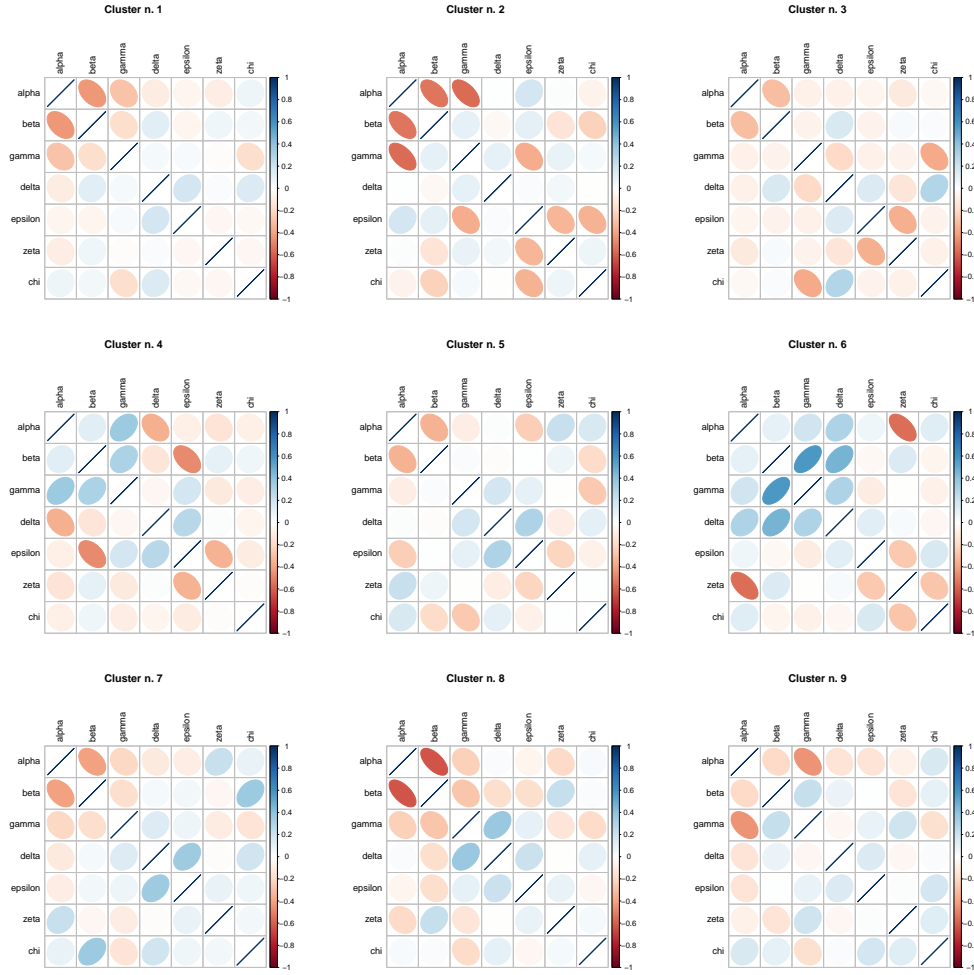


Figure SM-10: RNA data set. EM Estimated correlation matrix for clusters 1-9.

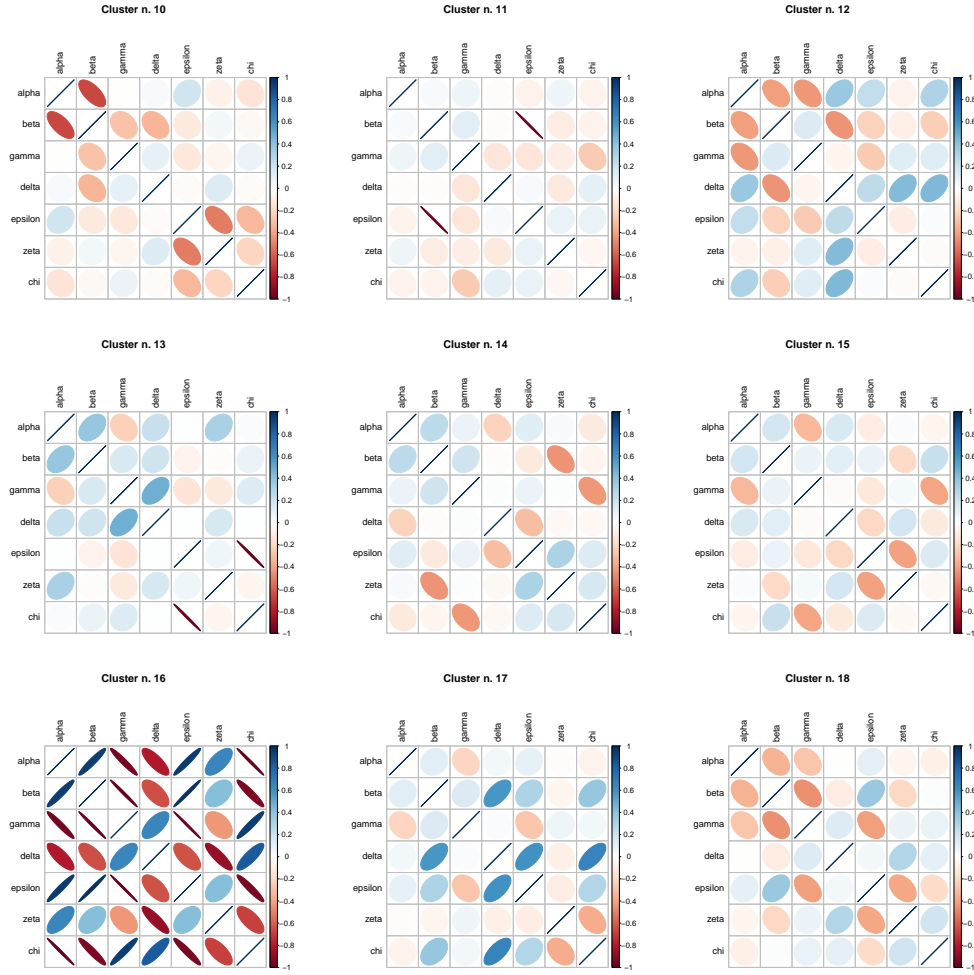


Figure SM-11: RNA data set. EM Estimated correlation matrix for clusters 10-18.



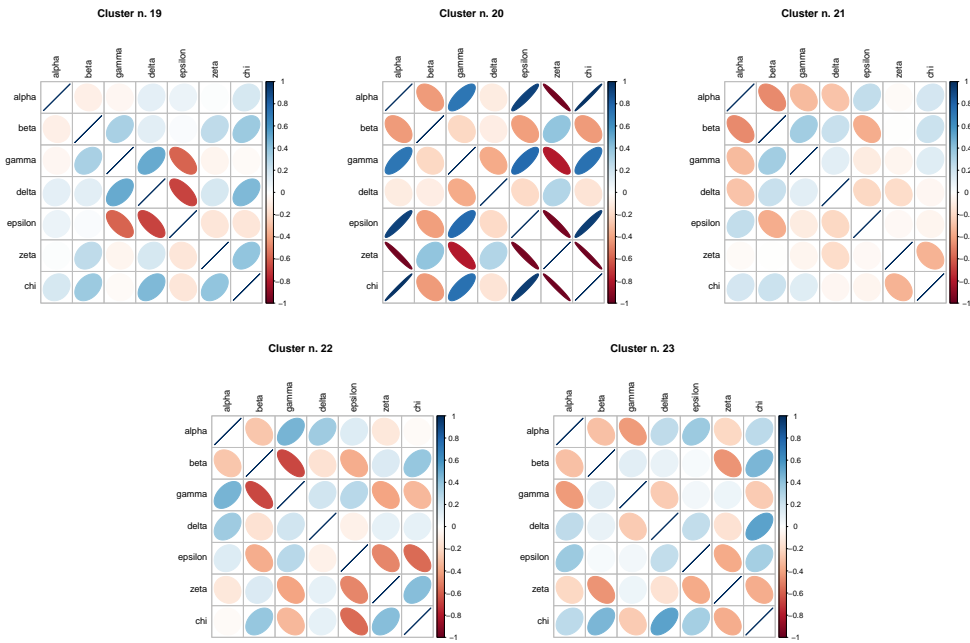


Figure SM-12: RNA data set. EM Estimated correlation matrix for clusters 19-23.

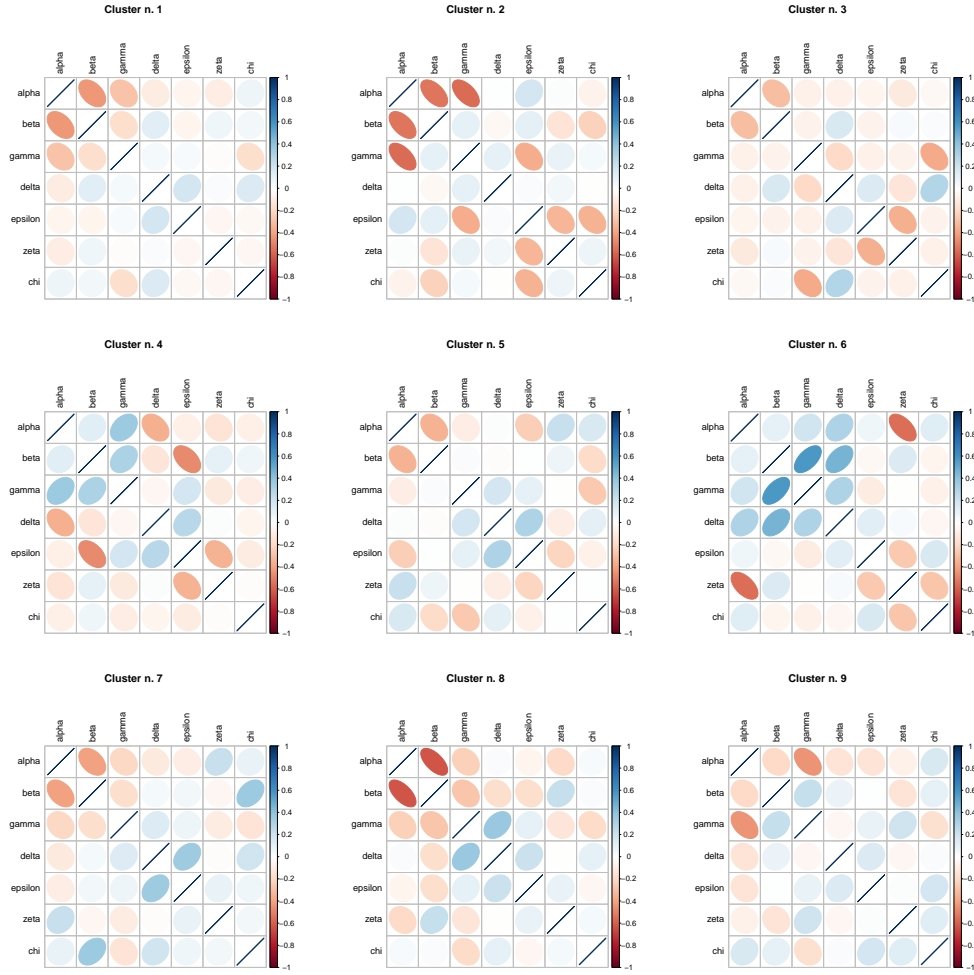


Figure SM-13: RNA data set. CEM Estimated correlation matrix for clusters 1-9.

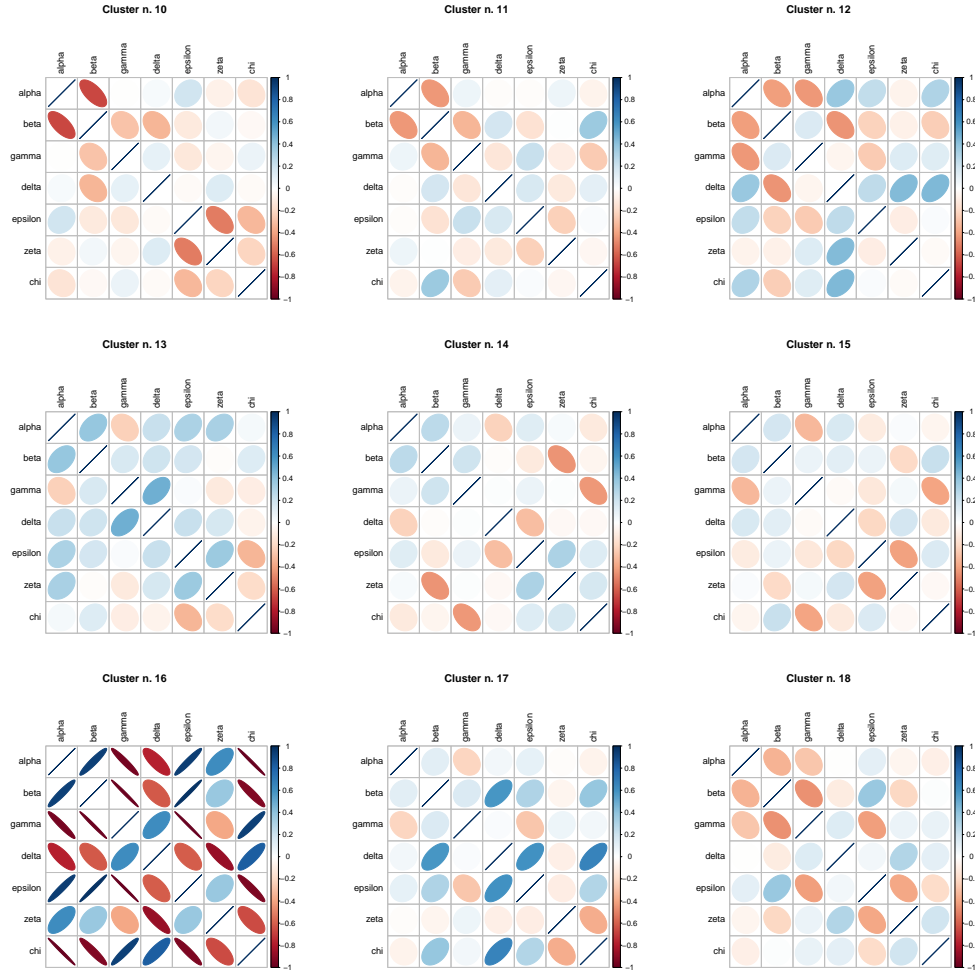


Figure SM-14: RNA data set. CEM Estimated correlation matrix for clusters 10-18.

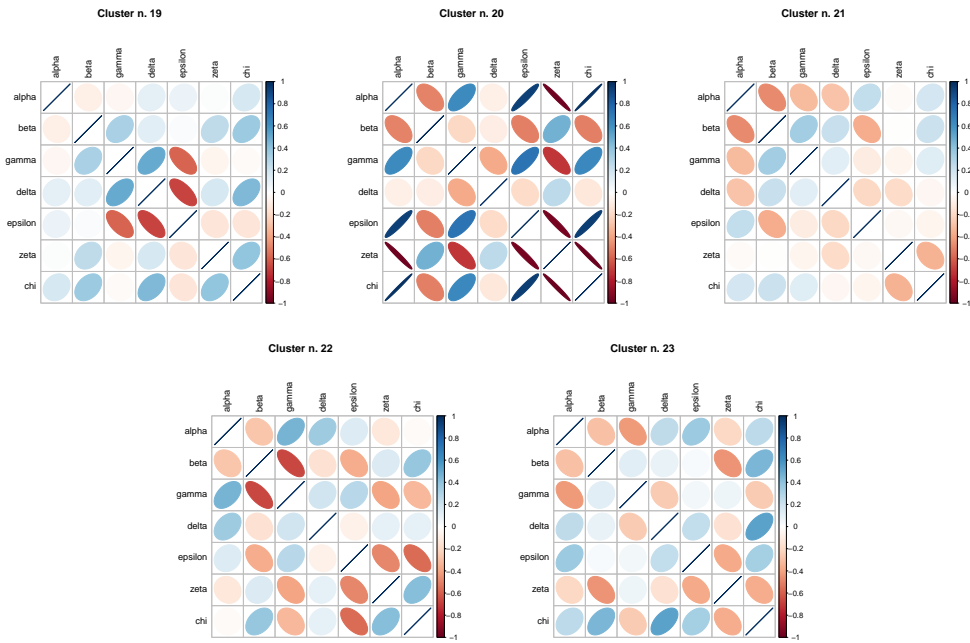


Figure SM-15: RNA data set. CEM Estimated correlation matrix for clusters 19-23.

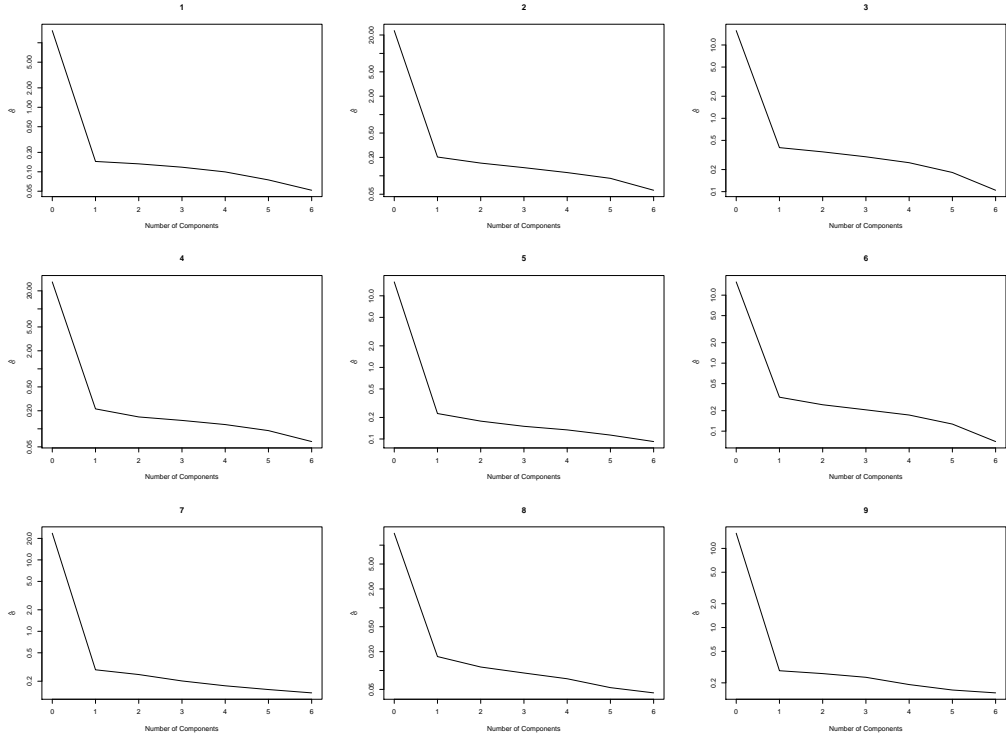


Figure SM-16: RNA data set. Estimated residual standard deviation as function of the number of components. Clusters 1-9.

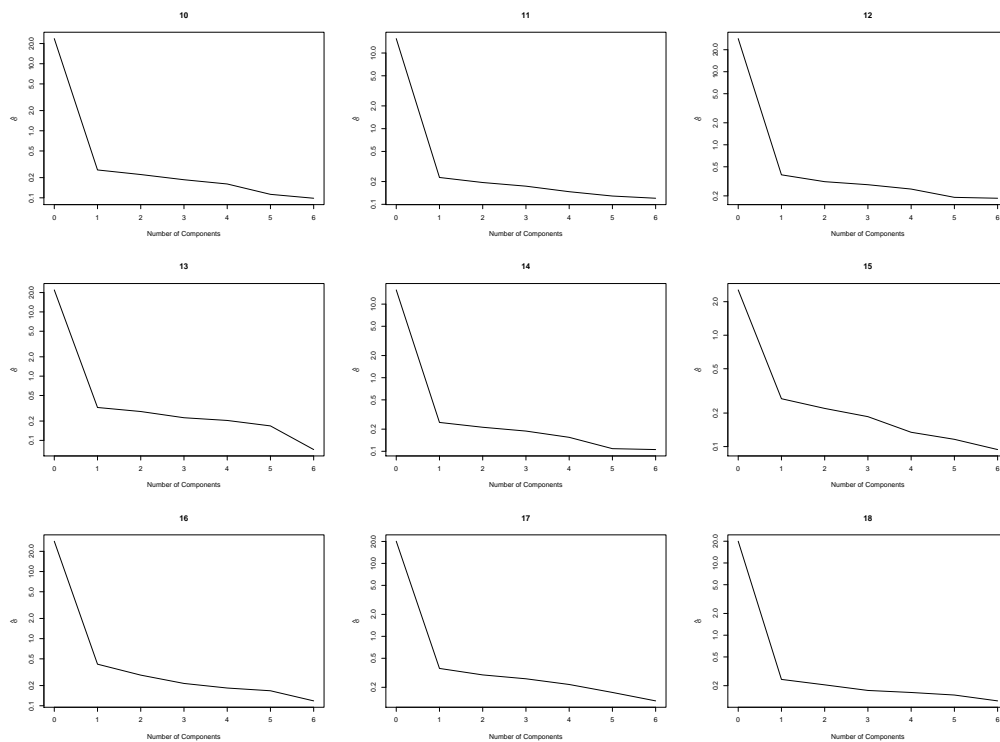


Figure SM-17: RNA data set. Estimated residual standard deviation as function of the number of components. Clusters 10-18.

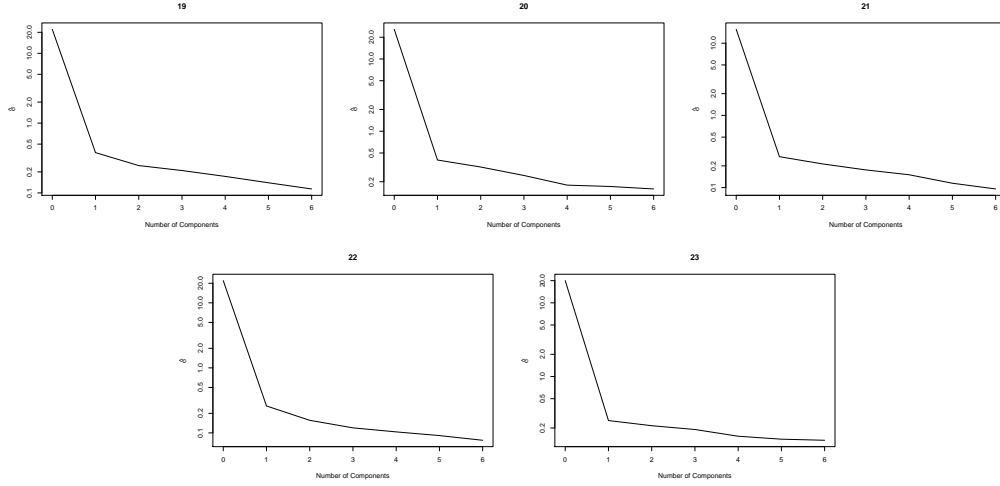


Figure SM-18: RNA data set. Estimated residual standard deviation as function of the number of components. Clusters 19-23.

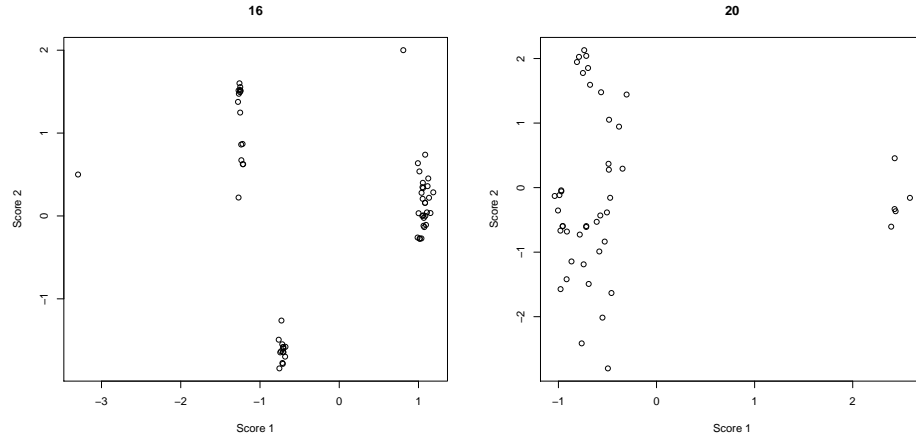


Figure SM-19: RNA data set. First two scores for cluster 16 (left) and cluster 20 (right).

Cluster #	# points	MSE			MAE			N. comp.		
		CV	KG	LRT	CV	KG	LRT	CV	KG	LRT
1	4917	12.208	12.194	12.192	3.151	3.151	3.151	1	4	5
2	477	21.761	21.745	21.728	4.128	4.128	4.128	1	2	5
3	232	11.919	11.882	11.839	3.118	3.118	3.118	2	3	5
4	211	31.582	31.560	31.544	4.577	4.577	4.577	1	2	5
5	140	8.628	8.606	8.586	2.578	2.578	2.578	1	2	5
6	139	5.916	5.871	5.832	2.172	2.172	2.172	1	2	5
7	139	22.376	22.325	22.308	3.982	3.982	3.982	1	3	5
8	138	10.695	10.695	10.687	2.979	2.979	2.979	2	2	5
9	128	12.077	12.021	12.012	3.148	3.148	3.148	1	4	5
10	122	20.832	20.856	20.799	4.078	4.078	4.078	2	1	5
11	85	15.253	15.242	15.229	3.641	3.641	3.641	2	3	5
12	84	18.686	18.686	18.622	3.559	3.559	3.559	2	2	5
13	79	10.284	10.254	10.231	2.971	2.971	2.971	2	3	5
14	72	11.486	11.486	11.454	3.068	3.068	3.068	2	2	5
15	60	9.308	9.308	9.274	2.844	2.844	2.844	2	2	5
16	60	12.918	21.013	13.779	2.712	3.585	2.756	2	1	3
17	59	27.650	27.650	27.590	4.210	4.210	4.210	2	2	5
18	54	12.235	12.220	12.220	3.159	3.159	3.159	2	3	3
19	52	35.179	35.179	35.137	5.131	5.131	5.131	2	2	5
20	46	5.473	5.288	4.654	1.895	1.864	1.766	2	1	4
21	35	23.472	23.455	23.438	4.164	4.164	4.164	2	3	5
22	33	8.108	8.108	8.092	2.559	2.559	2.559	2	2	4
23	28	9.926	9.926	9.926	2.715	2.715	2.715	2	2	2

Table SM-7: RNA data set. Performance of TPPCA and number of selected components by CV, KG and LRT.



## References

- H. Akaike. Factor analysis and AIC. *Psychometrika*, 52:317–332, 1987.
- A. Altis, P. Nguyen, R. Hegger, and G. Stock. Dihedral angles principal component analysis of molecular dynamics simulations. *Journal of Chemical Physics*, 26:244111.1–244111, 2007.
- M.S. Bartlett. Tests of significance in factor analysis. *British Journal of Psychology (Statistics Section)*, 3:77–85, 1950.
- A. Basilevsky. *Statistical Factor Analysis and Related Methods*. Wiley, New York, 1994.
- R. Bellman. *Adaptive Control Processes*. Princeton University Press, New Jersey, 1961.
- H. Bozdogan. On the frontiers of statistical modeling: An informational approach. *Proceedings of the first US/Japan conference*, 1994.
- J. R. Bunch and C. P. Nielsen. Updating the singular value decomposition. *Numerische Mathematik*, 31:111–129, 1978.
- J. R. Bunch, C. P. Nielsen, and D. C. Sorensen. Rank one modification of the symmetric eigenproblem. *Numerische Mathematik*, 31:31–48, 1978.
- R.B. Cattell. The scree test for the number of factors. *Multivariate Behavioral Research*, 1:245–276, 1966.
- G. Celeux and G. Govaert. A classification em algorithm for clustering and two stochastic versions. *Computational Statistics and Data Analysis*, 14: 315–332, 1992.
- B. Eltzner, S. Huckemann, and K.V. Mardia. Torus principal component analysis with applications to RNA structure. *Annals of Applied Statistics*, 2018. In press.
- P. T. Fletcher, C. P. Lu, S. Pizar, and S. C. Joshi. Principal geodesic analysis for the study of nonlinear statistics of shape. *IEEE Trans. Med. Imaging*, 23:995–1005, 2004.

- M. Frechet. Les elements aleatoires de nature quelconque dans un espace distance. *Ann. Inst. H. Poincare*, 10:215–310, 1948.
- L. Guttman. Some necessary conditions for common factor analysis. *Psychometrika*, 19:149–162, 1954.
- T. Hastie and W. Stuetzle. Principal curves. *Journal of American Statistics Association*, 84:502–516, 1989.
- K. Hayashi, P.M. Bentler, and K.H. Yuan. On the likelihood ratio test for the number of factors in exploratory factor analysis. *Structural Equation Modeling*, 14(3):505–526, 2007.
- H. Hotelling. Analysis of a complex of statistical variables into principal components. *Journal of Educational Psychology*, 24:417–441, 1933.
- S. Huckemann and H. Ziezold. Principal component analysis for Riemannian manifolds, with application to triangular shape spaces. *Advances in Applied Probability*, 38:299–319, 2006.
- J. Jackson. *A User’s Guide to Principal Component*. Wiley, New York, 1991.
- I. Jolliffe. *Principal Component Analysis*. Springer, New York, 2002.
- K.G. Jöreskog. Some contributions to maximum likelihood factor analysis. *Psychometrika*, 32:443–482, 1967.
- S. Jung, X. Liu, J.S. Marron, and S. Pizer. Generalized PCA via the backward stepwise approach in image analysis. *Brain, Body and Machine*, 83:111–123, 2010.
- S. Jung, I. L. Dryden, and J.S. Marron. Analysis of principal nested spheres. *Biometrika*, 99:551–568, 2012.
- H.F. Kaiser. The application of electronic computers to factor analysis. *Educational and Psychological Measurement*, 20:141–151, 1960.
- H. Karcher. Riemannian center of mass and mollifier smoothing. *Communications on Pure and Applied Math*, 30(5):509–541, 1977.
- W. J. Krzanowski. Cross-validatory choice in principal component analysis: Some sampling results. *Journal of Statistical Computation and Simulation*, 18:299–314, 1983.

- W. J. Krzanowski. Cross-validation in principal component analysis. *Biometrics*, 43:575–584, 1987.
- D.N. Lawley and A.E. Maxwell. *Factor Analysis as a Statistical Method*. Elsevier, New York, 1971.
- K.V. Mardia. *Statistics of Directional data*. Academic Press, London, 1972.
- K.V. Mardia, J.T. Kent, and J.M. Bibby. *Multivariate Analysis*. Academic Press, London, 1979.
- Y. Mu, P.H. Nguyen, and G. Stock. Energy landscape of a small peptide revealed by dihedral angles principal component analysis. *Proteins*, 58:45, 2005.
- A. Nodehi, M. Golalizadeh, and A. Heydari. Dihedral angles principal geodesic analysis using nonlinear statistics. *Journal of Applied Statistics*, 42:1962–1972, 2015.
- A. Nodehi, M. Golalizadeh, M. Maadooliat, and C. Agostinelli. Estimation of parameters in multivariate wrapped models for data on a p-torus. *Computational Statistics*, 2020. Accepted.
- V.M. Panaretos, T. Pham, and Z. Yao. Principal flows. *Journal of the American Statistical Association*, 109:424–436, 2014.
- K. Pearson. On lines and planes of closest fit to systems of points in space. *The London, Edinburgh and Dublin Philosophical Magazine and Journal of Science*, 2:559–572, 1901.
- X. Pennec. Intrinsic statistics on Riemannian manifolds: Basic tools for geometric measurements. *Journal of Mathematics and Imaging Vision*, 25:127–154, 2006.
- K.B. Petersen and M.S. Pedersen. *The Matrix Cookbook*. Technical University of Denmark, Denmark, 2012.
- S. Roweis. EM algorithms for PCA and SPCA. *Advances in Neural Information Processing Systems*, 10:626–632, 1998.

- K. Sargsyan, J. Wright, and C. Lim. Geopca: a new tool for multivariate analysis of dihedral angles based on principal component geodesics. *Nucleic Acids Research*, 40:25, 2012.
- G. Schwarz. Estimating the dimension of a model. *The Annals of Statistics*, 6:461–464, 1978.
- S.R. Searle. *Matrix Algebra Useful for Statistics*. Wiley, New York, 1982.
- F. Sittel, T. Filk, and G. Stock. Principal component analysis on a torus: Theory and application to protein dynamics. *Journal of Chemical Physics*, 147:244101.1–244101.12, 2017.
- M.E. Tipping and C.M. Bishop. *Probabilistic Principal Component Analysis*. Neural Computing Research, Aston University, Birmingham, 1997. Technical Report.
- M.E. Tipping and C.M. Bishop. Probabilistic principal component analysis. *Journal of the Royal Statistical Society*, 61:611–622, 1999.
- R. Vidal, Y. Ma, and S.S. Sastry. *Generalized Principal Component Analysis*. Springer, New York, 2016.
- S. Wold. Cross-validatory estimation of the number of components in factor and principal component models. *Technometrics*, 20:397–405, 1978.
- M. Zhang and P.T. Fletcher. *Probabilistic Principal Geodesic Analysis*. In Neural Information Processing Systems (NIPS), 2013. Nevada, United States.
- M. Zhang and P.T. Fletcher. Bayesian principal geodesic analysis for estimating intrinsic diffeomorphic image variability. *Medical Image Analysis*, 25:37–44, 2015.